Some Properties of Protactinium Metal and Its Compounds

By

Raymond Lloyd Dod

B.S. (Oregon State University) 1964
M.S. (University of California) 1970

DISSERTATION

Submitted in partial satisfaction of the requirements for the degree of

DOCTOR OF PHILOSOPHY

in

Chemistry

in the

GRADUATE DIVISION

of the

UNIVERSITY OF CALIFORNIA, BERKELEY

Approved:

.....

.....

.....

Committee in Charge

.....

SOME PROPERTIES OF PROTACTINIUM METAL AND ITS COMPOUNDS

Table of Contents

SOME PROPERTIES OF PROTACTINIUM METAL AND ITS COMPOUNDS

Raymond Lloyd Dod

Lawrence Berkeley Laboratory
University of California
Berkeley, California 94720

May 1972

Abstract

A modification of the usual metallothermic method of metal production is described, utilizing a molten salt crucible which substantially reduces the probability of contaminating the protactinium metal with crucible material. The method may have general applicability to the preparation of small quantities of high melting point metals.

A redetermination of the magnetic susceptibility of protactinium metal was made, resulting in a substantial change in value although not in temperature dependence from that previously reported. The new value is $(190 \pm 5) \times 10^{-6}$ cgs units/mole and is independent of temperature from ~7°K to 300°K. This value holds for both the normal tetragonal form of the metal and also the f.c.c. high temperature modification. The magnetic susceptibility of PaF_4 is also reported. The observed behavior can be interpreted to follow the Curie-Weiss law with an effective moment of 1.81 Bohr magnetons and a Weiss constant of 22.5°.

The reactions of protactinium metal with several common gases at temperatures up to 700° are described. Standard x-ray powder diffraction techniques were used to analyze the results. New compounds reported include two nitrides prepared by reaction of the metal with nitrogen

and with ammonia. Both exhibited a cubic fluorite type lattice. The observed lattice parameters were $a_o = 5.436 \pm 6$ Å and $a_o = 5.395 \pm 3$ Å. A new hydride structure for PaH_3 was observed, isomorphic with α-uranium hydride with $a_o = 4.152 \pm 2$ Å. Additionally, an unidentified phase was observed in reaction of hydrogen with Pa metal at 400°C, which was presumed to be a hydride since thermal decomposition regenerated the metal. The hydride previously reported for protactinium was not observed, nor was any evidence for the existence of the reported monoxide, PaO, seen in any reaction, including those with air, oxygen and water.

The melting point and thermal expansion coefficients for a high purity sample of the metal have shown that the previous values, derived from samples of dubious quality, were more accurate than had been thought.

INTRODUCTION

Although the element protactinium has been known radiochemically since 1913[1,2,3,4] and has been available in purified macroscopic quantities since 1927,[5] relatively little is known about this early member of the second "f" transition or actinide series. This is due to a number of factors; (1) the difficulty and expense of isolating the element, (2) the radioactivity associated with all isotopes of protactinium, making work in gloved enclosures mandatory, (3) the fact that much of interest in the general field of actinide chemistry has been associated with later members of the group, and finally (4) the difficulty of purification and general chemical intractability of the element. More recently, however, interest has been revived in the chemistry of protactinium because of the increasing attractiveness of using thorium in a breeder reactor for nuclear power applications. There is several times more thorium than uranium available in the earth's crust, and thus use of thorium in breeder reactors could yield considerably more fissionable material than could be obtained from uranium. In the reaction of thorium (^{232}Th, the only isotope naturally occurring to a significant level) with thermal neutrons, a high steady-state concentration of protactinium is built up

$$^{232}Th_{90}\ (n,\gamma)\ ^{233}Th_{90} \xrightarrow[22\ min.]{\beta^-}\ ^{233}Pa_{91} \xrightarrow[27d.]{\beta^-}\ ^{233}U_{92}.$$

Since the hazard potential of a nuclear reactor is very high, it is of great importance to understand and be able to predict the action of all chemical entities in the core region. Thus, a new importance has been placed upon deciphering the chemical and physical properties of protactinium

and its compounds.

Protactinium also commands interest because it is the first element of the actinide series which possesses one or more "f" electrons in stable oxidation states. As such it can be considered to be near the point at which the actinide series exhibits less of the character of a "d" transition series and more that of an "f" series.

The continuing actinide research program at the Lawrence Berkeley Laboratory, a portion of which is described here, is intended to provide information upon which conclusions can be based regarding the nature and behavior of these elements.

II. PREPARATION OF PROTACTINIUM METAL

A. Sources of Protactinium

^{231}Pa, the most stable isotope of protactinium, is a naturally occurring member of the 4n+3 radioactive series. It is the α-decay product of ^{235}U, and as such is found to about 0.2 - 0.3 parts per million of the amount of uranium present in uranium ores. The material used in this work was derived from "ethereal sludge" wastes left from the processing of high-grade pitchblende ores in Great Britain.[7] Approximately 105 g of protactinium was recovered by processing nearly 60 tons of "ethereal sludge", a recovery of greater than sixty percent of the total protactinium initially present. The method used, primarily using successive solvent extractions, is of limited general usefulness as the quality of uranium ore currently available is much lower; thus the protactinium is scattered in early processing of the ore.[7]

Protactinium can also be produced by neutron irradiation of thorium, but since thorium is present predominantly as ^{232}Th, the product is invariably mostly the short-lived β-emitting isotope ^{233}Pa if there has been no isotopic separation of the thorium. Since the protactinium produced in this way is rapidly self-contaminating with fissionable uranium, this is not the preferable isotope to work with, although the significance of protactinium today derives largely from this intermediate in the production of fissionable material for nuclear fuel from the relatively plentiful element thorium.

B. Purification

The primary contaminant in the protactinium recovered as described in the preceding section was approximately four percent niobium. Several

separations have been designed to remove niobium from protactinium, the most common being fractional crystallization of dipotassium fluoroprotactinate (K_2PaF_7) from aqueous HF solution[8] and anion exchange column separation.[9] Since the former method is quite time-consuming and is of generally poor yield, to say nothing of leaving the product as a difficultly soluble salt, the second method was used as the primary separation procedure in this work.

The ion exchange column separation (see Table 1) is relatively quick and additionally serves as a general clean-up operation as most common contaminants are eluted before the protactinium is stripped from the column, although thorium does elute with the protactinium, resulting in a detectable impurity in the radioactivity analyses, but generally not a chemically significant impurity since the thorium present is usually only the ^{231}Pa granddaughter, ^{227}Th, a short half-life isotope. A sample spectrographic analysis report for protactinium purified in this manner is given in Table 2.

Table 1. Ion Exchange Column Operation

Purpose: Separation of protactinium from niobium and other common contaminants.

Resin: Dowex 1×10, -400 mesh, F^- form.

Temperature: Room temperature.

Load: 2.5 - 3 M HF

Elution: 2.5 M high purity HF*, 3-4 column volumes.

Strip: 17 M high purity HF* (usually another 3-4 column volumes are necessary to recover most of the protactinium).

Remarks: Apparently any HF resistant material is satisfactory for the column. Chetham-Strode and Keller[9] used Kel-F; Lucite and polystyrene were used in this work. Cotton appears to be adequate material for the plug at the bottom of the column to prevent passing of resin beads.

*High purity HF was prepared using water from a two-stage quartz still[10] contained in a leached polyethylene centrifuge cone suspended in a closed container partially filled with commercial concentrated HF. Vapor equilibration for a period of months at room temperature was sufficient to bring the high purity HF to approximately 20 M.

Table 2. Sample Spectrographic Analysis of Protactinium Solution from Anion Exchange Purification.

Elements detected (μg per sample):

Pa (50), Si (0.05)

Elements looked for but not detected:

Al, Bi, Ca, Ce, Cr, Fe, Mg, Na, Nb, Ni, Sn, Ti, Y, Yb, Zr

*See Table 3, p. 9, for detection limits for these and other elements.

C. Assay and Analysis

In the process of purifying or otherwise manipulating materials, it is frequently desireable to know the quantities present in each of several fractions. Since weighing is frequently inconvenient, due both to the physical problems in safely weighing radioactive materials and to the usual lack of a compound of precisely defined stoichiometry, radioactive assay techniques are generally used. These methods utilize the fact that the decay rate of a radioactive isotope can be a precisely known quantity. The decay rate for ^{231}Pa is $1.062 \pm 0.0076 \times 10^{8}$ disintegrations per minute per milligram.[11]

The fastest, but least precise, method is γ-spectroscopy using a Li-drifted Ge gamma detector crystal. This technique can be applied to the radioactive substance in nearly any form which can be placed in front of the detector, is subject variation dependent upon that form. This is especially true in the case of ^{231}Pa wherein usually all γ peaks but the one at 27.3 keV are subject to interference from daughter activity. As a result, this assay technique is suitable only for following the bulk of the protactinium through a process.

A much better technique for α-emitters such as ^{231}Pa is that of α-counting and analysis. In this method, an aliquot of the radioactive material in solution is evaporated onto a counting planchet which can then be counted. In practice, gross counting was done in a 2π counter followed by α-spectroscopy using a Si surface-barrier detector in conjunction with a multichannel analyzer. This technique leads to quite accurate results, even with samples which are grossly contaminated with decay products,

since of all the decay products of ^{231}Pa, only ^{227}Ac has an α energy as low as its parent, and the α-branching ratio of ^{227}Ac is only 1.4%,[12] producing a possible error of less than 1% in most specimens unless there has been some enrichment of the Ac. Thus, since ^{231}Pa decays with a number of α-energies between 4.6 and 5.1 MeV, in general one can merely ascribe all α events of energy less than 5.1 MeV to ^{231}Pa, and all α events above that energy to daughter activity. This procedure only applies, of course, to ^{231}Pa samples which have been previously purified and have not since been contaminated with non-genetic isotopes.

A very significant error can occur in the preparation of assay planchets if they are prepared from hydro-halic acids, since the pentavalent compounds of Pa are volatile at the temperatures used in flaming the planchets. It has been usual practice in these studies to prepare planchets from sulfuric acid solutions, or to convert the sample to the sulfate before flaming.

Analysis for other than radioactive impurities was by copper-spark spectrographic analysis. This method gives quite satisfactory results; the limits of detection are given in Table 3. Protactinium has a very rich and intense emission spectrum and if a sample of greater than approximately 50 μg is used in a single analysis, the protactinium spectrum interferes with many lines used for quantitative determination of other elements, thus raising considerably the detection limits for those elements. Therefore, the usual practice was to limit the samples prepared to about 50 μg.

Table 3. Limits of Detection by Copper-Spark Spectrographic Analysis for Common Impurities.

Limit	Elements
0.01 µg	Ag, Al, Be, Ca, Cr, Eu, Fe, Ga, La, Mg, Mn, Mo, Nb, Ni, Sc, Si, Sr, Ti, V, Yb, Y, Zr
0.05 µg	Bi, Co, Er, Gd, Ge, Hf, Ho, In, Lu, Rh
0.1 µg	Am, Ce, Dy, Nd, Pb, Pd, Pt, Re, Sn, Ta, W, Zn
0.5 µg	As, Cd, Ir, Pr, U
1 µg	Au, Ba, K, Na, Sb

D. Metal Preparation

The purified protactinium from the ion exchange column was precipitated from solution by addition to aqueous ammonia prepared from doubly distilled water and gaseous ammonia in a polystyrene centrifuge cone. The precipitate was washed several times with ammonia solution, then allowed to dry under moderate heating, forming a dense pellet of hydrated protactinium oxide. The pellet thus produced was transferred to a platinum bucket and placed in a vacuum line made of nickel and monel (Fig. I). The line was evacuated and a flow of pure hydrogen started through the reaction chamber at a pressure slightly greater than one atmosphere. The hydrogen flow was continued, while the temperature was raised to 500°C and maintained for approximately 30 minutes. (This treatment served to partially reduce the oxide from the pentavalent state and thus minimized formation of volatile PaF_5.) The sample was then cooled in hydrogen to approximately 150°C and the flowing atmosphere changed to an approximate 50-50 mixture of HF and H_2. In this atmosphere, the temperature was again increased to about 600°C and maintained there for a period of several hours while an approximate thousand fold excess of HF was passed through the reaction chamber to completely convert the oxide to the tetrafluoride. The HF was then flushed from the chamber with flowing hydrogen and the sample was allowed to cool to room temperature in a hydrogen flow. The PaF_4 thus prepared was stored under vacuum until use in the metallothermic preparation of the metal. Although complete reduction of the pentoxide to the dioxide is not possible under the conditions specified above, sufficient reduction was achieved to limit losses due to volatilization of PaF_5 to less than about 10%.

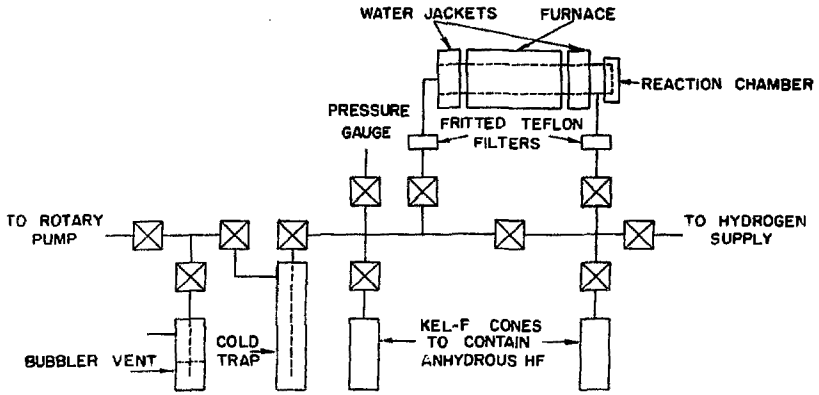

NICKEL-MONEL FLUORINATION VACUUM LINE

XBL 725-807

Fig. I

The metallothermic reduction of PaF_4 as previously executed at this laboratory utilized a method used successfully for the trans-plutonium actinides, with the actinide fluoride suspended in a spiral of small diameter wire being reduced by vapors of alkali or alkaline earth metals. The system used is shown in Fig. II. In this method, the system was heated above the melting point of the actinide metal either during or following reduction to allow agglomeration and to float the fluoride slag to the surface of the metal droplet which is retained by the wire spiral. Although tantalum wire proved adequate for the trans-plutonium actinides, protactinium at its melting point wet and apparently alloyed with the spiral; thus tungsten wire was used with some success. When one sample of Pa metal was prepared in a double loop of 0.001 inch tungsten wire, it proved impossible to recover the wire, except at the point of entry into the metal sample. Sectioning and polishing of the metal piece showed that the wire was definitely reduced in diameter at the entry point, and the wire had completely disappeared at points deeper in the protactinium. Contamination from this source could be held to a minimum by using very fine W wire and excising that section of the resultant Pa metal where the wire had been, as it was determined with the above-mentioned metal sample that the tungsten did not distribute itself evenly throughout the protactinium in the time the metal was kept molten. However, this method would have been very wasteful of material and was otherwise at least esthetically unacceptable.

Since the product metal must of necessity be in contact with the reductant metal fluoride slag, the possibility of using a crucible of

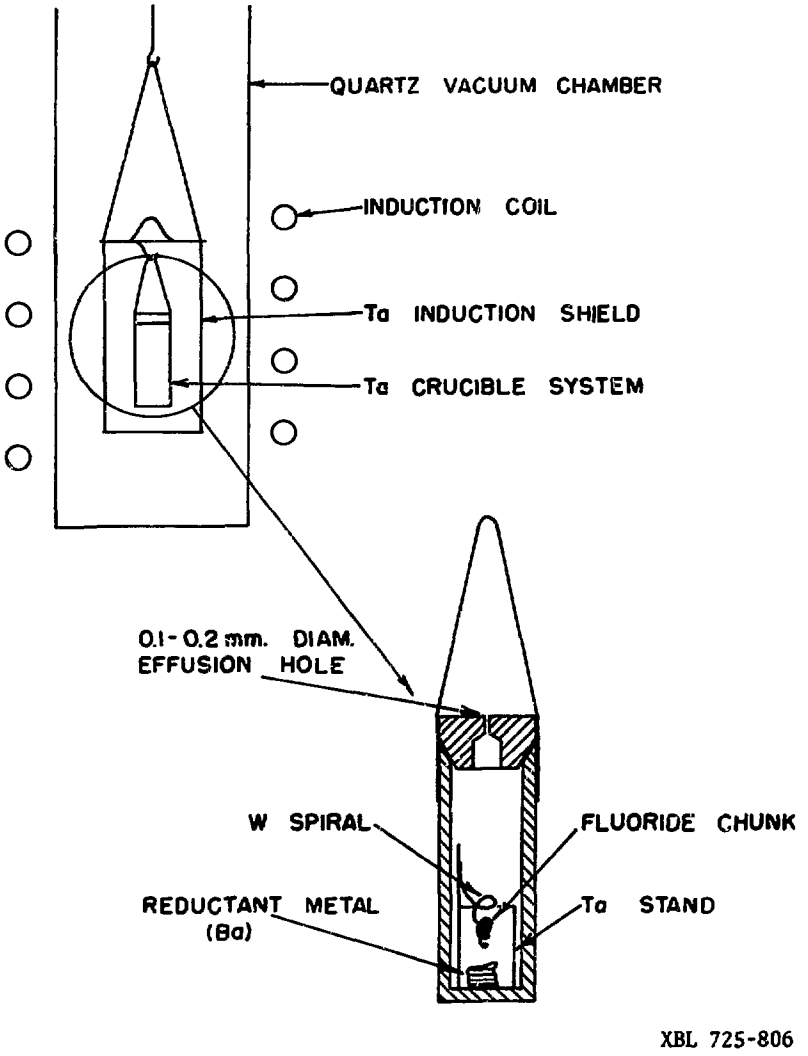

Fig. II. Old metal preparation apparatus.

of BaF_2 with a barium reduction was examined. It was first tried to use the heat generated by the reaction

$$2\ Ba + PaF_4 \longrightarrow Pa + 2\ BaF_2$$

to locally heat the Pa metal above its melting point of about 1565°C while maintaining the overall temperature of the system below the melting point of BaF_2 (1280°C). This proved to be impossible. A second possibility was to carry out the reduction of the PaF_4 to the metal in a BaF_2 crucible and then to raise the temperature of the entire system to a temperature above the melting point of protactinium, depending on the surface tension of the molten BaF_2 to contain the molten Pa metal. (This idea can be demonstrated simply by injecting a small amount of mercury into a drop of water suspended from the tip of a pipet.)

To the best of my knowledge, no determination of the surface tension of liquid BaF_2 at 1600°C has been made. Several experiments indicated that the maximum amount of BaF_2 which could be supported at that temperature by a band of 0.002 inch tantalum foil of about 5 mm diameter and 0.5 mm in height was about 200 mg. Assuming that the molten salt drop was supported by its surface tension at two interfacial contact rings with the metal band, and using the experimentally derived number of 200 mg, an effective surface tension can be calculated:

$$\gamma = \frac{mg}{2\pi R}$$

$$= \frac{(0.200)(980)}{4\pi(0.25)}$$

$$\approx 62 \text{ dyne-cm},$$

where m is the mass of the supported drop, g the acceleration due to

gravity, and R the radius of the support ring. Then, supposing the metal droplet within the molten salt drop to be supported by that same surface tension acting at a single interfacial ring of diameter equal to the maximum diameter of the droplet, and assuming a size of about 1.5 mm diameter for the droplet,

$$m = \frac{2\pi\gamma r}{g}$$

$$= \frac{2\pi(62)(0.075)}{980}$$

$$= 0.030 \text{ g},$$

where m is the maximum mass which a droplet of radius r can have and still be supported by the molten salt drop. If the liquid metal were of the same density as the room temperature tetragonal phase of the metal, a droplet 1.5 mm diameter would have a mass of 27.2 mg and should therefore be supported. In practice, no amount of metal in excess of about 15 mg has been prepared in any single reduction, and this has usually been adequately supported, ending up as a roughly spherical piece of metal at the bottom of the BaF_2 drop (see Fig. III).

The actual surface tension of BaF_2 at 1600°C is probably higher than the number derived above by a factor of two or more, since the other barium halide salts have surface tensions of 127-146 dyne-cm at temperatures twenty percent above their melting points[13] (absolute temperature - ∿ 1600°C for the corresponding BaF_2 number) and the surface tension increases with decreasing atomic number of the halide. This could imply that the above considerations are quite conservative from a theoretical point of view, but they have proven to be close to a practical limit.

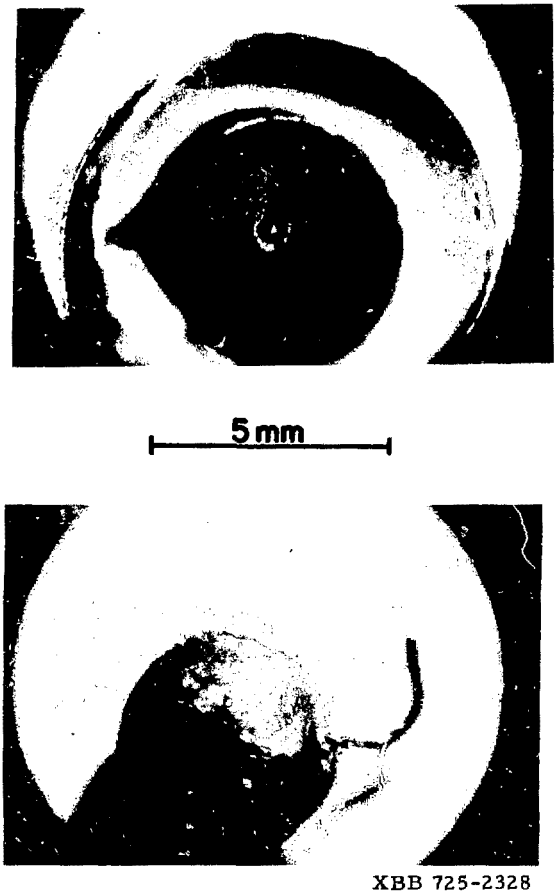

XBB 725-2328

Pa METAL IN BaF_2 CRYSTAL DROPS

Fig. III

This method of metal preparation was readily adapted to the existing system, replacing the stand supporting the spiral shown in Fig. II with a tantalum cylinder supporting inside it a small Ta ring holding the BaF_2 crucible. The details of the technique are given in the following section.

E. New Technique of Metal Preparation

From a large piece of optical quality single-crystal BaF_2 (Optovac, Inc.) a piece approximately 6 to 7 mm on a side is cleaved. This blank is then drilled with a solid carbide circuit board twist drill (typically #51, 1.7 mm diameter) to a depth of 3 1/2 to 4 mm. It is extremely important to execute this drilling operation slowly and to maintain a sharp cutting edge on the drill. A small lathe has proven adequate to provide the necessary control. The crucible blank is then mounted with a press fit on a piece of soft wood, the wood extending nearly to the bottom of the drilled cavity. The exterior of the crucible is then shaped with a carborundum disc to roughly the shape of a truncated one weighing approximately 170-175 mg (see Fig. IVa). In all machining operations on the BaF_2 crystal care should be taken to remove material slowly as fast cutting leads to local heat build-up and eventually to fracture. The most crucial stage is in the final shaping when the crucible walls are relatively thin and are very susceptible to fracture. Following final machining, the crucible is cleaned under a microscope to remove any residual adherent particles of BaF_2 or foreign material.

To support the crucible, a ring is formed from a strip of 0.002 inch tantalum foil which is about 1/2 mm wide. The ring necessary to

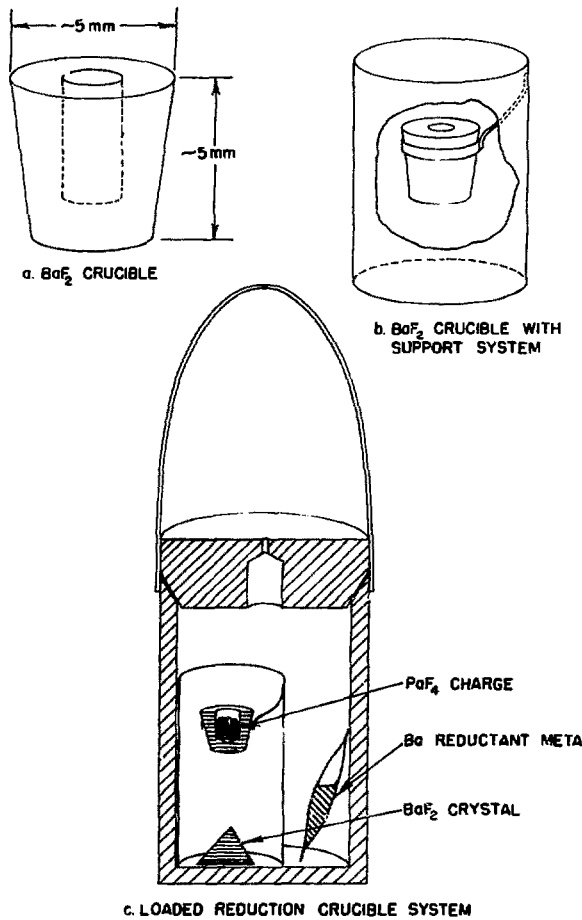

BaF_2 CRUCIBLE SYSTEM

XBL 725-801

Fig. IV

support crucibles as formed above is normally about 4.5 mm in diameter, the precise dimension being that which allows the crucible lip to project 1/2 to 1 mm above the ring when suspended in it. The ring is then spot-welded to a 0.010 inch tantalum wire which in turn is spot-welded to a cylinder formed of tantalum foil which serves as a support for the crucible (Fig. IVb). Following thorough cleaning of the tantalum parts in organic solvents and mineral acids, the crystal crucible system is assembled inside a tantalum crucible similar to that used in the former method, together with approximately 200 mg of additional BaF_2 (to minimize evaporative losses from the suspended droplet). The tantalum crucible is then hung in the usual manner inside a tantalum foil induction shield and heated inductively in high vacuum to 1000°C to thoroughly degas all surfaces.

After allowing the crucible system to cool in vacuum, it is disassembled leaving the BaF_2 crucible in its support ring. The crystal crucible is then loaded with PaF_4, compressed if necessary to achieve the desired size reduction product. A capsule of Ba metal (prepared by sealing a piece of Ba metal in a short length of thin-walled tantalum tubing in inert atmosphere by spot-welding both ends shut) is pierced with a tungsten needle and added to the Ta crucible (see Fig. IVc), and as quickly as possible the assembled system is returned to the vacuum line.

After pumping to a pressure of ≤ 1 μtorr, heating of the reduction crucible is begun, increasing the temperature slowly and maintaining the measured pressure at ≤ 10 μtorr. Heating in this manner is continued until noticeable amounts of barium metal begin to condense on the walls of the vacuum chamber, at which time the temperature of the Ta crucible is

raised to 1250-1275°C and maintained for 4-5 min. This reduces the PaF_4 to the metal, but does not agglomerate it. Large amounts of metallic Ba still remain in the crucible, so the temperature is reduced to ~1175°C and held constant for 1-1 1/2 hours. (For reductions on the milligram scale, reductant metal -- Ba -- excess of approximately ten-fold is used.) This length of time seems sufficient to generally remove all residual Ba metal from the BaF_2 crucible material. The temperature can then be raised to 1600°C for approximately 90 sec, melting the BaF_2 crucible and melting and agglomerating the Pa metal. The system is then allowed to cool in vacuum.

When the crucible system is disassembled, if all has gone well there is a resolidified drop of BaF_2 hanging in the Ta support ring with a small sphere of Pa metal at the bottom (bottom views of two such BaF_2 drops are shown in Fig. III). If the excess Ba metal has been baked from the system successfully, the drop will be colorless to yellow, and if not, the color will be bluish to gray. Figure III shows examples of both types of result. The yellow crystals show evidence of Pa^{4+} in their absorption spectra in the near infrared.[14] In either case, the metal may be chipped from the crystal by applying pressure to the regions adjacent to the metal sphere and it can then be cleaned by mechanically scraping with a sharp instrument. No sample of metal prepared in this manner has shown amounts of Ba detectable by copper spark spectrographic analysis; however, as noted earlier, the detection limit for Ba is rather high.

No quantitative data are available concerning the recovery efficiency of this method of metal preparation, however, metallic yields

have been estimated at $\geq$ 80% of the total fluoride loaded into the crucible. Losses can occur from protactinium salts dissolving in the BaF_2, molten metal contacting the tantalum ring and adhering, or failure of the BaF_2 drop to be supported. The second of these failures occurs only rarely, and the last obviously results in total loss of the sample.

III. MAGNETIC SUSCEPTIBILITY

A. Introduction

Magnetic measurements are of particular interest in the lighter members of the actinide series, since they often exhibit characteristics of both f and d transition elements. The magnetic behavior of protactinium metal has been reported by Bansal[15] to be temperature-independent paramagnetism between 20° and 300°K. Those results, however, are subject to question because of the low purity of his samples as indicated by the large degree of ferromagnetic impurity which he reported to be present. It was felt that those results could be considerably refined by repetition of the determination on samples of better known purity. Question also arises from the recent discovery of a second phase of protactinium metal,[16] insofar as a sizeable difference in atomic volume between the new face-centered cubic phase and the tetragonal phase has led to speculation of a different metallic valence for the newly discovered phase. Finally, speculation as to the electronic configuration of Pa^{4+} in pure compounds led to the efforts to check the magnetic susceptibility of PaF_4, a compound prepared intermediate in the process of making metal for other experiments.

B. Experimental

1. Principle of magnetic measurements.

The apparatus used in the magnetic susceptibility determinations reported here operates on the principle of the Faraday balance. A modification suggested by Cunningham[17] wherein the force exerted on the sample by the magnetic field is balanced by the force of gravity operating

on the same sample allows this method to be used for the measurement of small magnetic susceptibilities of very small samples.

In the traditional Faraday balance, the sample is suspended from a balance of some sort in a magnetic field which has a sharp field gradient in the vertical direction with a gradient very much less in the horizontal plane such that the sample has exerted on it a force in the vertical direction, either up or down depending upon the magnetic character of the sample and the direction of the field gradient. This force can then be directly measured on the balance from which the sample is suspended. This method is obviously limited by the load capacity and sensitivity of the balance, and is generally not applied when the force measured on the sample is less than hundredths or even tenths of dynes.

The Cunningham modification rotates the magnet pole-piece caps such that the direction of maximum field gradient is in a horizontal direction, perpendicular to both the magnet axis and the direction of the gravitational force. In this orientation, the force applied to the sample by the magnetic field in essence rotates the sample in an arc centered at its suspension point. The forces acting on the sample with such an arrangement are shown in Fig. V. The force due to the magnetic field (parallel to the direction of the field gradient), F_1, is balanced by the forces F_2 and F_3, operating respectively on the sample (and its container) and the suspension fiber.

At equilibrium, the net torque on the system is zero, and assuming the fiber to be infinitely flexible,

$$F_2 d + F_3\left(\frac{d}{2}\right) - F_1 L\cos\theta = 0 \qquad (1)$$

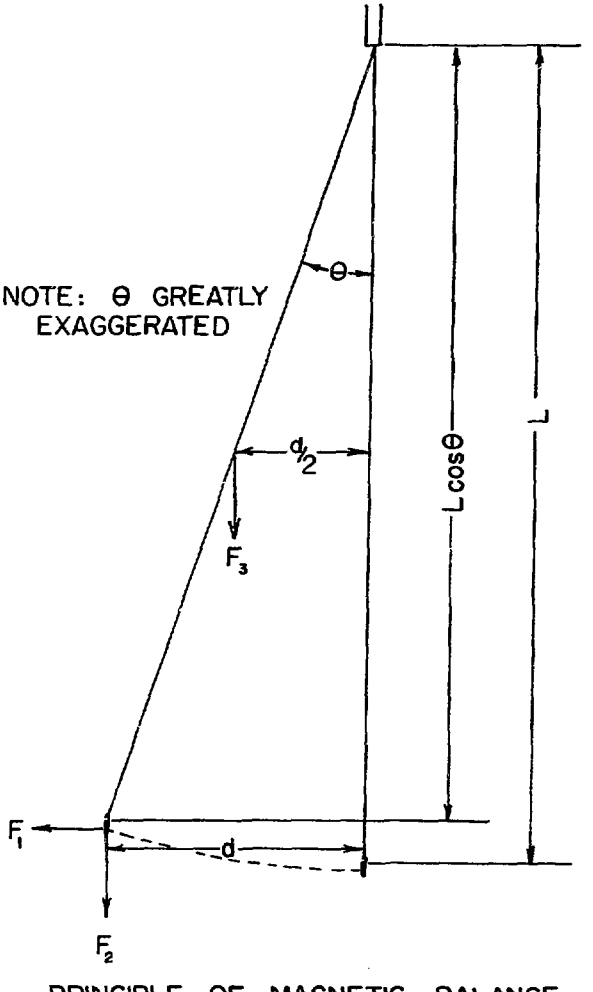

PRINCIPLE OF MAGNETIC BALANCE

XBL 725-805

Fig. V

or

$$F_1 L\cos\theta = F_2 d + F_3\left(\frac{d}{2}\right), \qquad (2)$$

where

$$F_1 = (m_h\chi_h + m_{sc}\chi_{sc} + m_s\chi_s)\,\mathcal{H}\frac{\partial\mathcal{H}}{\partial x}$$

$$F_2 = (m_h + m_{sc} + m_s)g$$

$$F_3 = m_f g$$

and

L = length of suspension fiber

d = deflection of the sample due to magnetic field

g = acceleration due to gravity

m_h = mass of hook on fiber

m_{sc} = mass of sample container

m_s = mass of the sample

m_f = mass of the suspension fiber

$\mathcal{H}$ = magnetic field strength at the sample position

$\frac{\partial\mathcal{H}}{\partial x}$ = magnetic field gradient in the direction of sample displacement at the sample position

χ_h = gram susceptibility of the hood

χ_{sc} = gram susceptibility of the sample container

χ_s = gram susceptibility of the sample.

Inserting these terms into the equilibrium expression (Eq. (2)),

$$(m_h\chi_h + m_{sc}\chi_{sc} + m_s\chi_s)\,\mathcal{H}\frac{\partial\mathcal{H}}{\partial x}L\cos\theta =$$

$$(m_h + m_{sc} + m_s + m_f/2)dg. \qquad (3)$$

Since many of these quantities can be difficult to determine separately, it is in practice convenient to combine them as a single constant, K, which is a characteristic of the apparatus and can be determined through calibration with a standard substance. K is defined for convenience of calculation as

$$K = \frac{\beta}{L\mathcal{H}(\partial\mathcal{H}/\partial x)} . \qquad (4)$$

Further simplification of eq. (2) can be achieved by considering the angle, θ, and its cosine. Although the magnet pole pieces are designed to achieve a relatively large volume of constant $\mathcal{H}(\frac{\partial\mathcal{H}}{\partial x})$, the sharpness of the field gradient makes this volume much smaller than might be desireable, and thus the constancy of the product $\mathcal{H}(\frac{\partial\mathcal{H}}{\partial x})$ is guaranteed by returning the sample to a fixed null position by translating the suspension point, using a micrometer control. The limit of travel of this suspension system defines the maximum angle which the fiber can make with respect to the vertical. Since paramagnetic effects are usually larger than diamagnetic ones, the null position is chosen such that there is approximately three times as much travel in the direction to restore a paramagnetic deflection as to restore a diamagnetic one. This travel of approximately 0.75 cm brings the fiber support ring into contact with the wall of the evacuable chamber in which it is supported. If, at the maximum travel, the sample is restored to its null position, the angle θ will be 1.07°, the cosine of which is 0.99982. If, then, in the above equations cosine θ is set equal to unity, the maximum error which could result would be less than 0.02%. Since the known variation in magnetic susceptibility of the calibrating substance is greater than this by

approximately two orders of magnitude, the assumption that cosine θ equals unity is deemed to be acceptable.

Using this assumption and gathering the several quantities into the apparatus constant, K, eq. (2) becomes

$$(m_h\chi_h + m_{sc}\chi_{sc} + m_s\chi_s)\left(\frac{g}{K}\right) = (m_h + m_{sc} + m_s + m_f/2)dg \qquad (5)$$

or, the gram susceptibility of the sample is

$$\chi_s = \frac{(m_h + m_{sc} + m_s + m_f/2)Kd}{m_s} - \frac{m_h\chi_h + m_{sc}\chi_{sc}}{m_s} . \qquad (6)$$

By deleting the presence of the sample (m_s, χ_s) in the above argument and following a similar procedure,

$$m_h\chi_h + m_{sc}\chi_{sc} = (m_h + m_{sc} + m_f/2)Kd_o \qquad (7)$$

where d_o is the deflection which would be measured of an empty sample container. Making this substitution in eq. (6),

$$\chi_s = \frac{(m_h + m_{sc} + m_s + m_f/2)Kd}{m_s} - \frac{(m_h + m_{sc} + m_f/2)Kd_o}{m_s} . \qquad (8)$$

This expression allows the gram susceptibility of the sample to be calculated from measured (and calculated) weights, measured deflections of the full and empty sample container, and an apparatus constant which can be determined by use of a standard substance whose susceptibility is well known.

2. Construction of apparatus.

The apparatus designed on the above principles and used in this study is shown in Fig. VI. It is capable of making measurements on samples ranging from fractions of a microgram to tens of milligrams, the upper limit being primarily a function of available space in the sample tube and the lower limit being determined by the finite mass of a containment system for any sample. In general, the sample container is chosen to match not only the physical size of the sample, but also the expected magnetic susceptibility. Thus, a sample of low susceptibility would require a lighter container than one of high susceptibility in order that reasonable deflections (d) might be observed. For example, the protactinium metal samples used in this study were expected to be of low susceptibility, and thus containers of minimum weight were desired. Knowing that the minimum deflection which can be measured with this apparatus is approximately 2.5 μ, the minimum detectable force on the sample can be calculated. For example, the second metal sample has a mass of 0.479 mg and its container 1.008 mg. From eq. (2)

$$F_1 L\cos\theta = F_2 + F_3 \frac{d}{2} = (m_h + m_{sc} + m_s)gd + m_f g\frac{d}{2}$$

$$F_{1min} = \frac{(m_h + m_{sc} + m_s + m_f/2)gd_{min}}{L\cos\theta}$$

$$= \frac{((0.0644 + 1.008 + 0.479 + 0.080)\times 10^{-3})gd_{min}}{40}$$

$$= 1.01 \times 10^{-5} \text{ dyne.}$$

This minimum detectable force is approximately ten times larger than that

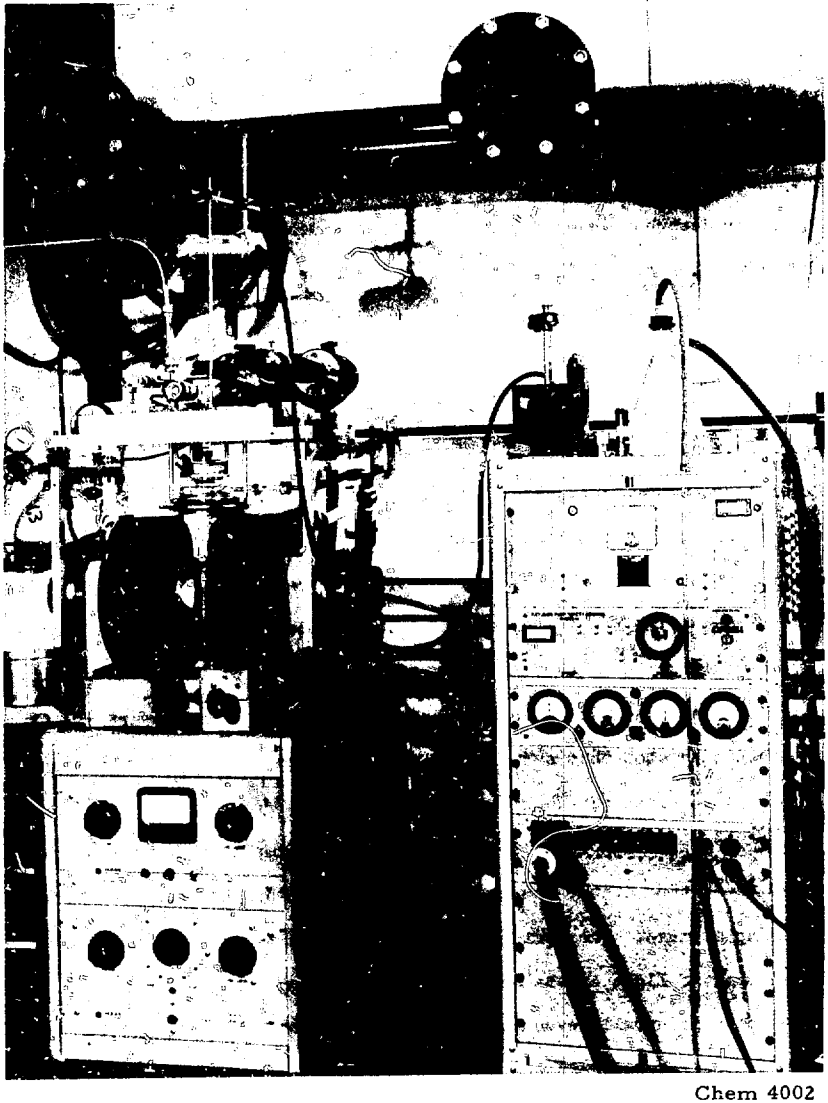

Fig. VI. General view of the magnetic susceptibility apparatus.

calculated by Fujita[26] for a sample smaller by three orders of magnitude. As can be seen in the above calculation, the minimum force measureable is approximately $1/10^5$ of the combined weight of the sample and containment-suspension system. Also, a change in weight of the system (due to adsorbed or desorbed gases for example) by as much as one percent will change the observed deflection by only the same percentage.

A sketch of the sample tube and micrometer-controlled suspension assembly is shown in Fig. VII. A piece of Dural tubing, A, containing a micrometer adjusted platform on a shaft is mounted atop the tube on plate I. On the adjustable platform rides a brass ring, C, containing the fiber suspension point. From this ring, a fused silica fiber, M, hangs down into a quartz tube, L, supporting the sample container, Q, at the desired point between the magnet poles. The brass ring, fiber and sample can be removed as a unit for changing the sample. The top of the assembly is sealed with a quartz plate, and the interior of the Dural housing and quartz tube can be evacuated through valve, E. A front-surface mirror is positioned atop this assembly to allow indirect viewing of the sample through the telescope visible in Fig. VI. The mirror has a hole through its center, allowing light from a sodium-vapor lamp to illuminate a mirror, S, at the bottom of the sample tube, providing a bright background for the sample image. The sodium-vapor lamp is used to provide intense monochromatic light as the optics of the telescope are not achromatic. The system is usually evacuated and flushed with dry helium several times to minimize residual condensible gases in the sample area. Measurements are made with 1/3 atmosphere of dry helium in the quartz tube to facilitate

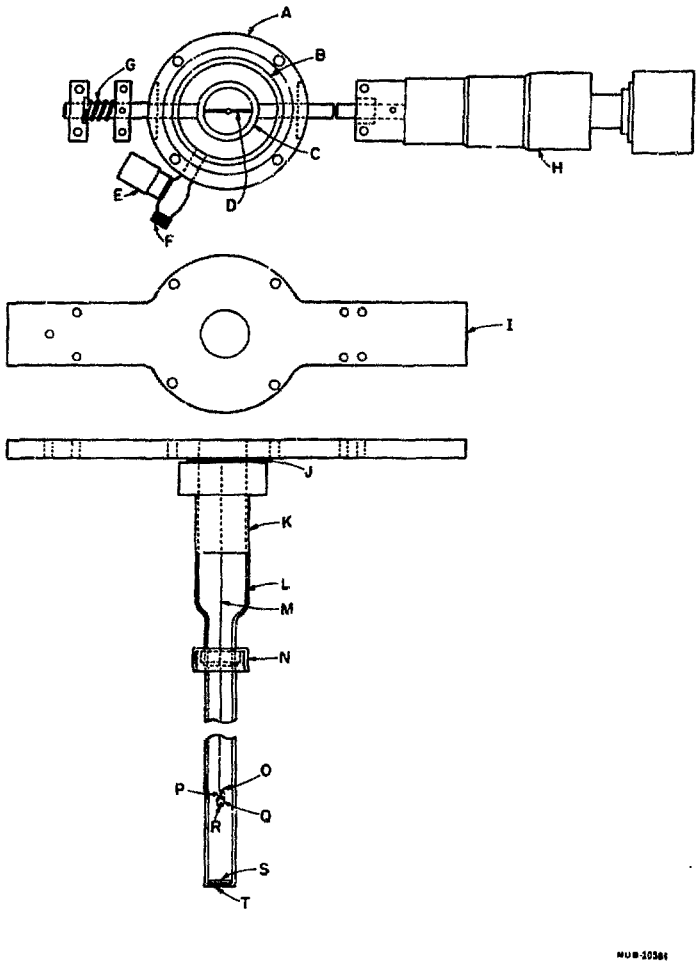

Fig. VII. Magnetic susceptibility sample tube and translation system.

temperature equilibration with the coolant fluids outside the quartz tube. In general, when the image of the sample is aligned with an adjustable hairline in the eyepiece of the telescope, a precision of 2.5 μ (0.10 micrometer division) is attained in making measurements of sample displacement.

To allow low temperature measurements to be made, the sample tube is mounted within a dewar system which is sketched in Fig. VIII. Because of the physical constraints of the magnet gap, it is of two-walled construction, although a copper finger, F, reduces substantially the temperature gradient near the inner wall of the dewar. The effect, however, is not sufficient to allow containment of liquid helium within the dewar, thus the lower limit of approximately 7°K was present for all measurements made. Liquid coolants with boiling points greater than or equal to that of liquid nitrogen are introduced into the dewar through an opening at A while liquids colder than that are transferred directly into the bottom of the dewar through a vacuum-jacketed stainless steel transfer tube, G. The dewar system is mounted on an adjustable metal platform which can be moved both horizontally and vertically to achieve optimum positioning of the sample with respect to the magnet pole faces.

The magnet is a Varian Model 4004 electromagnet with an air gap of 4 inches. Current-regulated power is furnished to the magnet windings by a V2300A power supply and a V2301A current regulator, the combination capable of providing up to 4 amperes of power regulated within 0.1% with line voltage and load resistance fluctuations of up to 10%.

3. Calibration of apparatus.

Since, as has been mentioned, it is very difficult, if not

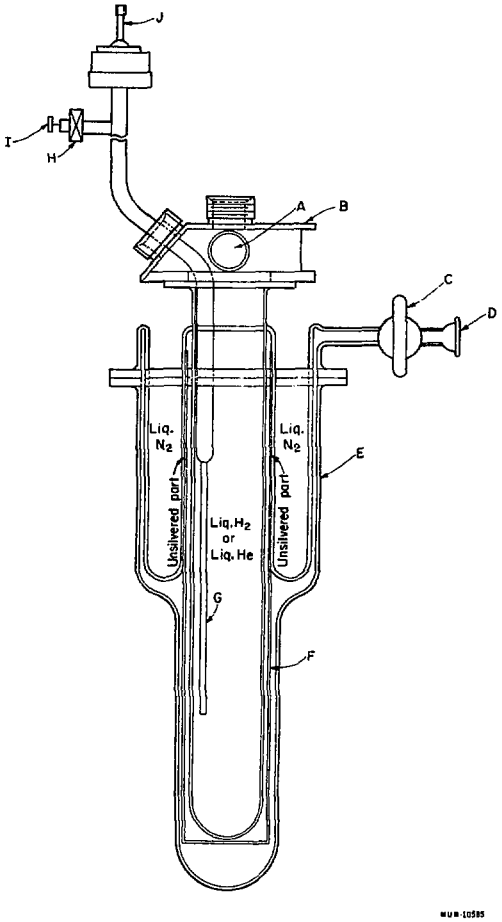

Fig. VIII. Magnetic susceptibility dewar system.

impossible, to determine all quantities in eq. (3), a reverse procedure, measuring displacements of a sample of known susceptibility allows evaluation of the constant, K. It is convenient to determine this constant for a number of magnetic fields, or, in terms of a more readily measured quantity, current through the magnet windings.

All calibrations in this study were with nickelous ammonium sulfate hexahydrate ($Ni(NH_4)_2(SO_4)_2 \cdot 6H_2O$, Baker and Adamson lot #7) as a standard. The magnetic susceptibility of this compound has been determined by Cossee[51] to be

$$\chi_g[Ni(NH_4)_2(SO_4)_2 \cdot 6H_2O] = \left(\frac{3174}{T + 2.5} - 0.30\right) \times 10^{-6} \text{ cgs}$$

with a deviation between different preparations of about two percent.

Calibration procedure was as follows:

(1) A fused silica sample container was prepared and thoroughly cleaned to remove any magnetic impurities by leaching in hot HCl for several hours.

(2) The hook and fiber were carefully measured with a microscope and their weights calculated using the density of fused quartz as 2.30 g/cm^3.

(3) A ball of Apiezon W wax sufficient to seal the opening of the tube prepared in step (1) was prepared by gently heating a small fragment of the wax which had been cut to size using non-magnetic instruments. This ball was carefully pressed onto the opening of the sample container and the whole assembly weighed to ±2 μg on an Ainsworth model FH microbalance.

(4) The sample container was then loaded onto the fiber and placed in the magnetic balance. The image of the sample container was

then aligned with the moveable hairline in the filar micrometer eyepiece of the telescope.

(5) A series of measurements was made, recording the micrometer travel necessary to restore the sample container to its null position at each half-ampere increment from 1.5 to 4.0 a of magnet coil current. A minimum of three readings were taken at each current setting, and the average value of the differences between the readings with the magnet on and magnet off taken as the displacement of the empty sample container, d_o.

(6) A similar set of measurements was taken at 77.4°K, and the absence of temperature dependence of displacement values was taken to mean that the sample container was free of para- and ferromagnetic impurities. (If temperature dependence had been noted, steps (3) through (6) would be repeated until it was removed.)

(7) The sample container was removed from the apparatus and loaded with an amount of $Ni(NH_4)_2(SO_4)_2 \cdot 6H_2O$ sufficient to make measured displacements at 4.0 a and 77.4°K near the maximum measureable. The sample container was then sealed by gently heating the wax sphere until it melted, forming an air-tight seal at the top of the sample container. The loaded sample container was then weighed, again to ±2 μg.

(8) A series of measurements was made as described above at each of two temperatures, usually room temperature and liquid nitrogen temperature. A third or fourth temperature, intermediate between those two, was often checked to provide additional data.

Applying eq. (8) at each temperature, T_1 and T_2,

$$\chi_{s1} = \frac{(m_h + m_{sc} + m_s + m_f/2)Kd_1}{m_s} - \frac{(m_h + m_{sc} + m_f/2)Kd_o}{m_s}, \quad (9)$$

$$\chi_{s2} = \frac{(m_h + m_{sc} + m_s + m_f/2)Kd_2}{m_s} - \frac{(m_h + m_{sc} + m_f/2)Kd_o}{m_s}. \quad (10)$$

Solving eqs. (9) and (10) for the apparatus constant, K,

$$K = \frac{m_s(\chi_{s2} - \chi_{s1})}{(m_h + m_{sc} + m_s + m_f/2)(d_2 - d_1)}. \quad (11)$$

Typical values of K and approximate values for $\mathcal{H}$ and $\frac{\partial \mathcal{H}}{\partial x}$ are shown in Table 4.

4. Temperature control and limits.

The sample temperatures below room temperature were achieved either by filling the dewar with a coolant at its normal boiling or melting point under atmospheric pressure, or by passing chilled gas through the dewar at a temperature above its boiling point. The former method is more convenient, but certain temperature regions of interest cannot be covered adequately in this manner. Several coolants of the first type used with this apparatus are the following:

Coolant System	Temperature, °K
Ice-water	273.2
Monochlorodifluoromethane (Freon-22)	232.2
Dry ice-acetone	194.7
Carbon tetrafluoride (Freon-14)	145.0
Liquid methane	111.7
Liquid oxygen	90.2
Liquid nitrogen	77.4
Liquid hydrogen	20.4
Liquid helium	4.2

Table 4. Typical Calibration Data for Magnetic Susceptibility Apparatus.

Magnet Current, a	$\mathcal{H}^a$, g	$\frac{\partial \mathcal{H}^b}{\partial x}$, $\frac{g}{cm}$	$K \times 10^8$ c
4.0	4890	1270	1.068 ± 9
3.5	4560	1160	1.243 ± 14
3.0	4090	1050	1.524 ± 12
2.5	3500	898	2.069 ± 21
2.0	2790	736	3.098 ± 79
1.5	2140	540	5.637 ± 252

[a]Measured with a Model 720 Rawson-Lush Rotating Coil Gaussmeter (Rawson Electrical Equipment Co., Cambridge, Mass.). This is only an approximate value as the gaussmeter sensing coil occupied a volume ~25 times larger than the sample container.

[b]Calculated from eq. (4) using measured K and approximate field strength values.

[c]Averages based on four independent calibrations using four different temperatures. Error limits are standard deviations. The units of K are defined by eq. (11).

Several of these coolant systems were not used in the current studies because of lack of facilities for safely exhausting the boiled-off gases. Also, liquid helium proved to be impossible to use, as mentioned above, because of the limitations of the dewar.

Temperatures between ~7° and ~40°K were achieved by transferring liquid helium at varying rates through a vacuum-jacketed stainless steel transfer tube. A Nullmatic Pressure Regulator, Model 40-7, with a pressure range of 0 to 0.5 atm was found to be an adequate control in pressurizing the liquid helium dewar to control the rate of transfer. Temperatures could generally be controlled within ±0.5°K for approximately 1/2 hour.

Thermometric measurements were made with several instruments. The temperatures of the several coolant systems were checked with a platinum resistance thermometer and the temperatures of the coolant in the dewar (down to liquid nitrogen temperature) was monitored with an iron-constantan thermocouple the calibration of which had been checked against a platinum resistance thermometer. Below liquid nitrogen temperature, a carbon composition resistor was used as a temperature sensing device. The resistor was calibrated down to liquid helium temperature with a Model 1417 Solitron germanium resistance thermometer, and had a satisfactory temperature coefficient of resistance from approximately 40°K down to 4°K to allow the temperature to be determined to ~±0.1°K. Since the helium flow cryostat system could not be stabilized above approximately 35°K, this proved to be an adequate range.

5. Magnetic measurements.

Making magnetic susceptibility measurements on a specimen of unknown susceptibility involves steps similar to those delineated for calibration of the apparatus. As previously mentioned, the size and weight of the sample container is determined by the physical size and the expected magnetic behavior of the sample. In general, one adjusts the mass of the container to allow deflections to be as large as possible but still allow measurements to be taken at maximum field strength at all temperatures at which measurements are to be made. Since most substances of magnetic interest are paramagnetic in nature, and paramagnetism is usually temperature dependent, the maximum deflections are usually noted at the lowest temperatures. When the sample is very small or of very low susceptibility, this consideration is usually inconsequential since the containers cannot feasibly be made light enough to exhibit the maximum measureable deflection.

Ferromagnetic impurities in the samples or sample containers can have a significant effect on the results even when present in extremely small quantities. However, if the impurity is not of an amount to totally overwhelm the magnetic behavior of the pure sample, a correction can be made for its presence. Since paramagnetic effects in a non-uniform field are proportional to $\mathcal{H}\frac{\partial \mathcal{H}}{\partial x}$ and ferromagnetic effects when saturated in a strong magnetic field are proportional to only $\frac{\partial \mathcal{H}}{\partial x}$, the presence of field dependence of susceptibility of the sample is an indication of ferromagnetic impurity.[18] The observed magnetic susceptibility of the sample, $\chi_{\mathcal{H}}$, can be expressed as

$$\chi_{\mathcal{H}} = \chi_o + \frac{c}{\mathcal{H}} \qquad (12)$$

where χ_o is the susceptibility of the pure substance and c is a constant characteristic of the saturated ferromagnetic impurity. From eq. (12), it can be seen that as the field strength becomes very large, the observed susceptibility is nearly equal to the actual susceptibility of the pure substance. Therefore, if a plot is made of $1/\mathcal{H}$ vs χ for a given temperature, the value of χ at $1/\mathcal{H} = 0$ should be equal to the actual value of the susceptibility of the pure sample. Such plots are easily made, but require a number of measurements to be made at any single temperature in the case of samples with temperature-dependent susceptibility.

C. Results and Discussion

1. The magnetic susceptibility of protactinium metal.

Two specimens of protactinium metal showed a small temperature-independent paramagnetism between ~7° and 298°K. Although this behavior is of the same type as that reported previously,[15] the value of the susceptibility observed in these measurements was lower by nearly 30%. The results of this investigation are shown in Fig. IX and Table 5, together with the results previously reported.

The metal specimens used in this study were from two separate preparations, although they trace back to a common initial ion exchange purification. They were treated separately from the precipitation of the protactinium hydroxide onward. Each was prepared using the barium fluoride crucible technique. All measurements were made with samples contained in light quartz buckets capped with a small ball of quartz which had been partially coated with Apiezon W wax. Sample #1 was an elongated piece of metal cut from a disc which had been formed from a

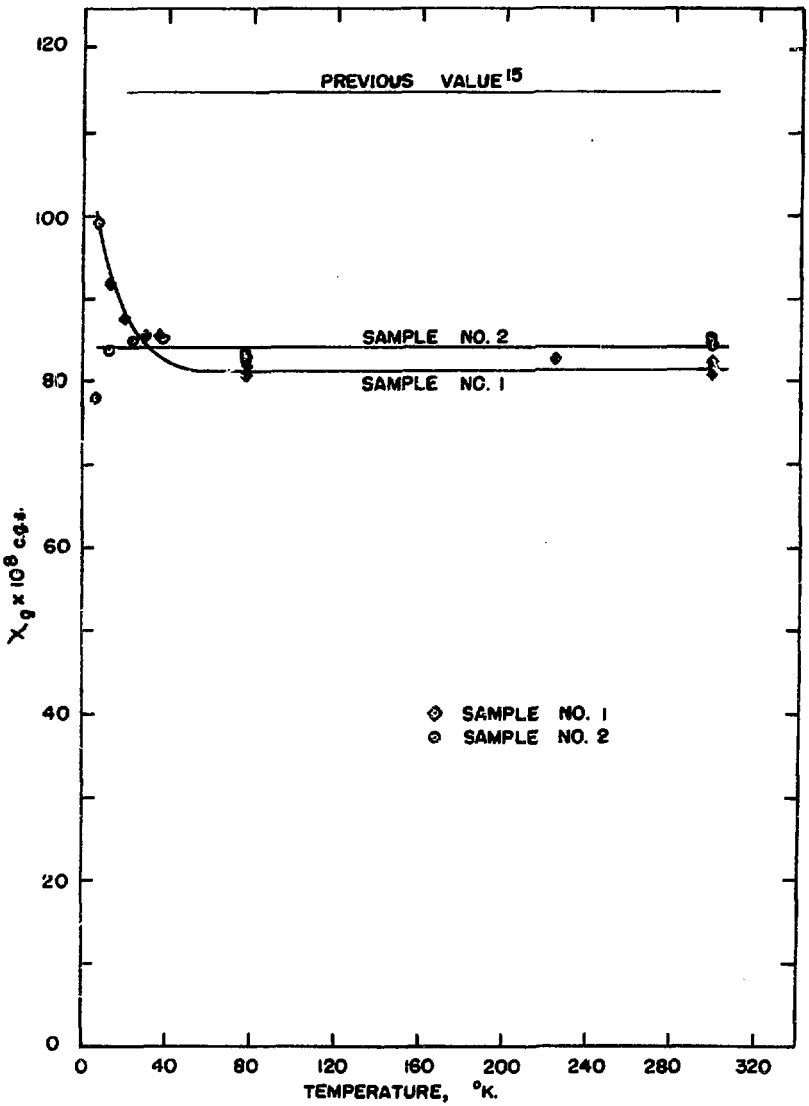

Fig. IX. Magnetic susceptibility of protactinium metal.

Table 5. Magnetic Susceptibility of Pa Metal

	χ_g, gram susceptibility $\times 10^8$	χ_M, molar susceptibility $\times 10^6$	Temperature range
Sample #2	82.9 ± 2.0	191 ± 4.6	6.7 - 298°K
Sample #1	82.0 ± 2.8	189 ± 6.5	20.0 - 299°K*
Bansal (15)	116.1 ± 6	268.2 ± 14	20 - 298°K

*The measured values below 20°K have been neglected because of non-linearity for reasons mentioned in the text.

spherical reduction product totaling approximately 6 mg. To avoid ferromagnetic contamination, the pressing operation was carried out with the protactinium metal ball between sheets of tungsten foil, and the cutting operation with small scalpels formed from tungsten rod. Sample #2 was used as prepared, a small sphere which had been cleaned by scraping with a tungsten needle.

Because of the very low susceptibility of the protactinium metal, it was desireable to have the sample containers as light as possible. By drawing quartz tubing of outside diameter of about 0.6 mm, with wall thickness of about 1/20 that value, containers of approximately 1/2 mg weight were manufactured. Adding the sealing plug - necessary for reasons of safety in dealing with radioactive material - brought the total mass of the containment system to slightly more than one milligram in each case. The total masses of the containment systems and the masses of the samples are shown in Table 6.

Pieces of about 20 μg each were cut from the samples after the magnetic measurements for x-ray diffraction analysis. Sample #1 proved to exhibit only the pattern of the normal tetragonal metal, with no lines which could not be indexed as belonging to that phase. Sample #2 showed the tetragonal phase amounting to an estimated 70% of the total, the remainder being the face-centered cubic phase reported recently.[16] Since this phase is unstable at room temperature, and cold-working of the metal tends to cause it to transform to the tetragonal phase, the 30% figure would represent a lower limit on the total amount of f.c.c. phase present in the undisturbed sample which was used for the magnetic measure-

Table 6. Masses of Pa Metal Magnetic Susceptibility Samples and Sample Containers.

	Mass of Sample Container	Mass of Sample
#1	1.131 mg	0.950 mg
#2	1.008 mg	0.479 mg

Table 7. Spectrographic Analysis of Pa Magnetic Susceptibility Samples.

Elements detected, μg per sample:

Sample #1		Sample #2		Acid*	
Ca	<0.01v	Ca	0.01	Ca	0.01
Mg	0.01	Mg	≤ 0.01	Mg	0.05
Si	0	Si	≤ 0.01	Si	0.02
Pa	50	Pa	100	Pa	0

Elements looked for but not detected:**

Ag, Al, Am, As, Au, Ba, Be, Bi, Cd, Ce, Co, Cr, Dy, Er, Eu, Fe, Ga, Gd, Ge, Hf, Ho, In, Ir, K, La, Lu, Mn, Mo, Na, Nb, Nd, Ni, Pb, Pd, Pr, Pt, Re, Rh, Sb, Sc, Sn, Sr, Ta, Th, Ti, U, V, W, Yb, Y, Zn, Zr

v = visible

*HCl-HF acid mixture used to dissolve the metal. Analysis is of approximately the same amount used to prepare the metal spectrographic samples.

**See Table 3 for limits of detection for these elements.

ments. In reality, the actual figure is probably considerably higher, since the cutting of a second x-ray analysis sample from the same piece of metal produced a sample with no appreciable sign of the f.c.c. phase.

Pieces of 50-100 μg were cut from each piece and dissolved for copper spark spectrographic analysis; the results are shown in Table 7 together with the results of an analysis of the acid mixture used to dissolve the samples.

As mentioned above, the sample containers were capped with quartz balls which had been partially covered with Apiezon W wax. Considerable care is necessary in both the initial covering of the quartz ball by gently heating it and in the thermal softening of the wax when sealing the plug to the sample container as the wax evidently can produce paramagnetic impurities if overheated. This problem can usually be minimized if the wax is not heated so intensely that it flows freely. The effect of overheating is shown in Fig. X as the temperature dependence of the magnetic susceptibility at low temperature of the empty sample container used for metal sample #2. The susceptibility of the sample container used for metal sample #1 was not measured below 77°K since it showed no significant temperature dependence to that temperature and the effect observed later was not known. Comparison of the effect noted at low temperature in the empty (and later loaded) sample container for sample #2 with the low temperature deviation from temperature independence of sample #1 reveals striking similarities, and since no reasonable physical explanation would seem to account for such behavior of the metal, this deviation below ~20°K has been attributed to the container rather than

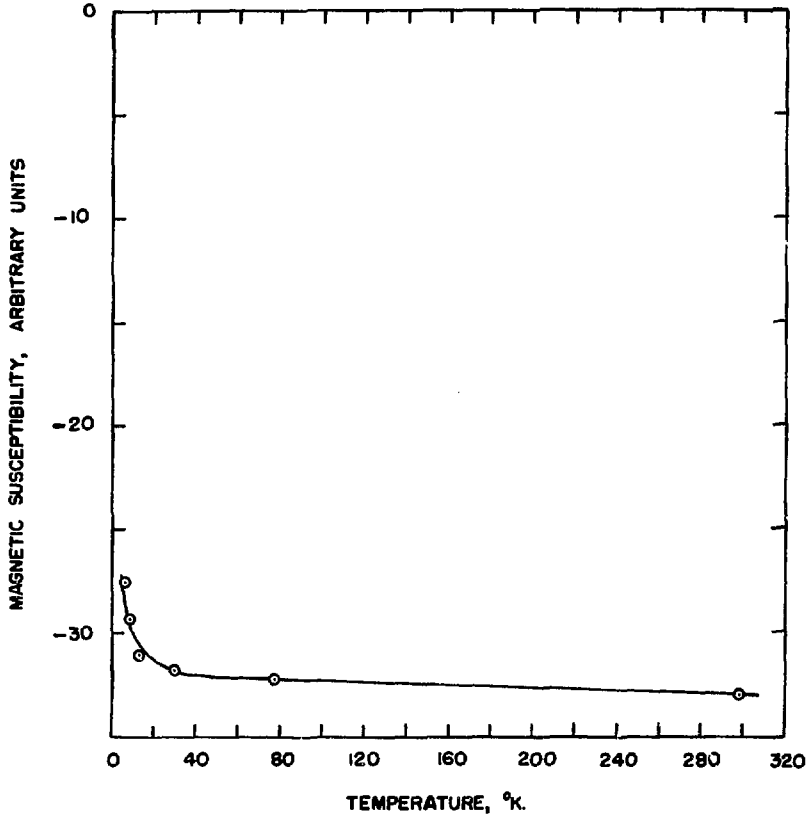

Fig. X. Magnetic susceptibility of empty sample container including wax-covered plug.

the protactinium.

Each sample of metal showed a small amount of field dependence of susceptibility. The method described in the preceding section was applied to the data to correct for ferromagnetic impurity. The corrected values for the susceptibility of the metal were lower than the raw values by approximately 5%. A calculation shows that the observed ferromagnetism could be caused by as little as 1.2 ppm of iron in the metal sample if it were present in ferromagnetic domains. The limit of detection for iron by the copper spark spectrographic analyses is approximately 500 ppm, or about 0.2 mole%; thus a small amount such as would be necessary to cause the observed magnetic effect could easily be present.

2. The magnetic susceptibility of protactinium tetrafluoride.

Two determinations were made of the magnetic susceptibility of protactinium tetrafluoride as a function of temperature from room temperature down to near the temperature of liquid helium. The samples used were from different purification cycles, and were very different in physical appearance, representing the extremes of color which have been observed. Although both preparations yielded the characteristic x-ray powder diffraction pattern of PaF_4,[19] sample I was a very dark reddish brown while sample II was very light gray, nearly white. The powder patterns of each showed only lines which could be indexed on the basis of the monoclinic unit cell reported by Stein. The complexity of the pattern beyond $2\theta = 60°$ did not warrant indexing beyond that point.

The samples were each contained in a quartz sample container, open at the top in the case of sample I and sealed except for a small gap with an Apiezon W-coated quartz ball in the case of sample II. (It

might be noted that the weight of the sample container for sample I was insufficient to allow measurements to be made below 15°K, a lower limiting situation often encountered in making measurements on paramagnetic substances.)

A linear least squares fit of the data collected from both samples (Table 8) leads to a curve which follows the Curie-Weiss law with a Weiss constant, Δ, of 22.5° and an effective moment, μ_{eff}, of 1.81 Bohr magnetons. While within experimental error for the linear fit, the data seems to better fit a curve as shown in Fig. XI, a curve which is consistent in shape with that found in the other $5f^1$ compounds UCl_5 (Ref. 20) and NpF_6 (Ref. 21) (See Fig. XII). The magnetic behavior of $PaCl_4$ (Ref. 22), also shown in the same figure, is irregular and as such is not strictly comparable.

The structure of PaF_4 is complex,[55] with two different types of metal ions, each surrounded by an irregular polyhedron consisting of eight fluorine nearest neighbors, and as such it is subject to significant and anisotropic crystalline field effects, making further interpretation of the data impossible without supplementary information.

Table 8. Experimental Data for Magnetic Susceptibility of PaF_4.

Sample I - dark material		Sample II - light material	
T, °K	$\chi_g \times 10^6$, cgs units*	T, °K	$\chi_g \times 10^6$, cgs units*
296.4	4.52	297.8	4.73
235	5.28	297.7	4.70
145	7.77	77.4	13.42
77.4	12.99	77.4	13.45
33.1	25.21	77.4	13.48
15.5	49.68	37.4	21.75
		22.8	32.55
		7.5	59.9

*Corrected for the diamagnetic susceptibility of ThF_4. (Ref. 52)

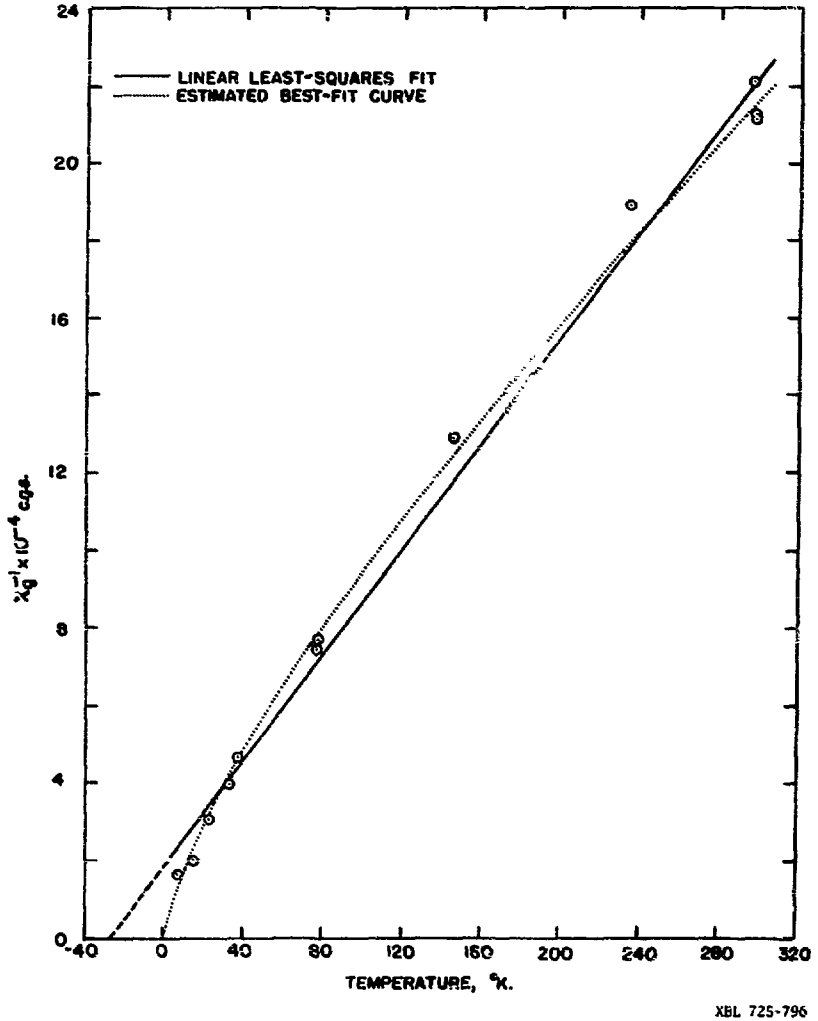

Fig. XI. Magnetic susceptibility of PaF_4.

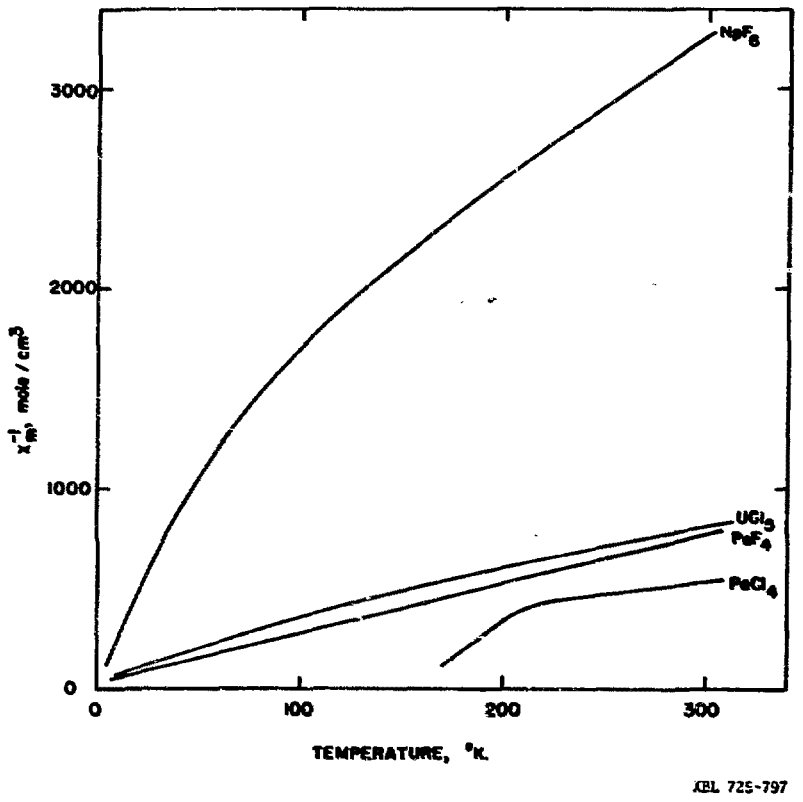

Fig. XII. Magnetic behavior of several $5f^1$ halide compounds.

IV. REACTION OF PROTACTINIUM METAL WITH COMMON GASES

A. Introduction and Apparatus

In handling a metal in normal atmospheres and in preparation of compounds, it is convenient to know something of the chemical behavior of the metal with common gases. It is with the intent of determining such behavior for protactinium metal that the following series of experiments was initiated.

It was decided that the reaction of protactinium metal with common gases should be carried out for a sequence of temperatures with each gas. Since the compounds resulting would probably in some cases be reactive towards the laboratory atmosphere, any manipulations of the reacted metal would have to be performed in the reactive atmosphere, inert atmosphere or vacuum. The total amount of protactinium available for these experiments was limited, only a few milligrams of pure metal being prepared, with a reserve stock of a few hundred milligrams of impure protactinium oxide. It was decided that the reaction of metal pieces of 20 to 40 μg each directly in x-ray capillaries would provide a reasonable degree of safety and minimize transfers of radioactive material. This amount of protactinium could also be safely handled in a high-draft fume hood, where all manipulations would be very much more simple than in a glove box.

The reaction of a solid sample with a gas in a thin x-ray capillary has become relatively common practice, and several workers[23,24,25,26] have shown this to be a practical method with very small (<1 μg) samples which are unstable in room air, although the possibility of diffusion of

oxygen or water vapor through a thin-walled quartz capillary has been mentioned.[26] The use of larger samples, tens rather than tenths of micrograms, allows the capillary wall thickness to be increased without serious degradation of the quality of the x-ray powder diffraction patterns due to random scattering of x-rays from the quartz. The thicker capillaries reduce the possibility of diffusion of gases through the walls, if indeed this is a problem, and also provide an additional safety factor through their greater mechanical strength.

To seal the capillary from the external atmosphere during x-ray exposures, a stopcock was fitted to the capillary, allowing the specimen to be isolated in vacuum or any desired atmosphere. The stopcock system used (Fig. XIIIa) was developed by Parsons and Cunningham[27] and was initially described by Copeland,[25] who reported it to be incapable of isolating samples from the laboratory atmosphere. Experimentation showed this defect to stem from two possible sources -- the failure of the greased joint at the stopcock and the diffusion of air through the thin-walled capillary. The latter of these possible sources of leakage was minimized as described above by increasing the thickness of the capillary walls, and unsuccessful attempts were made to avoid the former by careful lapping of the joint after it was modified. Although this improved the system, channelling, or leakage through the grease, persisted with all manner of vacuum and stopcock lubricants tried. Since the stopcock joint was capable of holding for a few tens of minutes to hours at a time, it was decided that a second standard taper piece inserted in the end of the stopcock and then sealed off under vacuum (see Fig. XIIIb) would provide a sure seal for the periods necessary to obtain x-ray

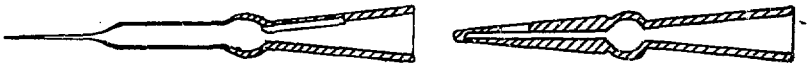

a.

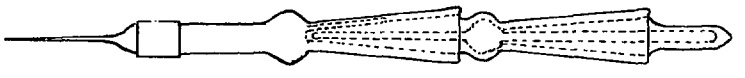

b.

"STOPCOCK" CAPILLARY SYSTEM

XBL 725-803

Fig. XIII

diffraction photographs while allowing reconnection to the preparative vacuum line for further reaction of the sample.

The metal used for the reactions was prepared by metalothermic reduction with barium of a pellet of PaF_4 suspended in a double loop of 0.001 inch tungsten wire. The resultant metal piece was cleaned by scraping with a tungsten needle and a fine scalpel point, and the outer portions which had been in contact with the tungsten wire were trimmed away. Although tungsten was observed to dissolve in the molten protactinium, a copper-spark spectrographic analysis of the metal used in these experiments showed no detectable tungsten (see Table 9). Apparently the amount of time that the metal was held in the molten state was insufficient to allow all the tungsten wire to dissolve and distribute itself throughout the protactinium droplet.

Each reaction sample was cut from the large piece of metal in an argon-filled inert atmosphere box and placed into a capillary which had been checked for vacuum integrity and degased at 500°C for 1 hour while under high vacuum. The loaded capillary was then transferred to the preparative vacuum line and evacuated. When a pressure of approximately 1 μtorr was reached, the metal sample and the surrounding area of the capillary were heated to 500°C for 1 hour while the high vacuum in the capillary was maintained through continuous pumping. The sample was then allowed to cool and was sealed off in high vacuum to permit its identity to be determined by x-ray diffraction prior to the commencement of reaction.

The reactions were carried out with the sample mounted on the preparative vacuum line sketched in Fig. XIV. This line was constructed

Table 9. Spectroscopic Analysis of Metal Used in Reaction Studies.

Elements detected (amount in μg):

Pa (50), Mg (0.05)*

Elements looked for but not detected:**

Al, Bi, Ca, Cr, Fe, La, Mn, Na, Ni, Pb,

Si, Sn, Ta, Th, Ti, W, Yb, Y, Zn, Zr

*The magnesium is probably due to finely powdered MgO dispersed in the glove box during polishing of a metal specimen.

**See Table 3, p. 9, for detection limits for these elements.

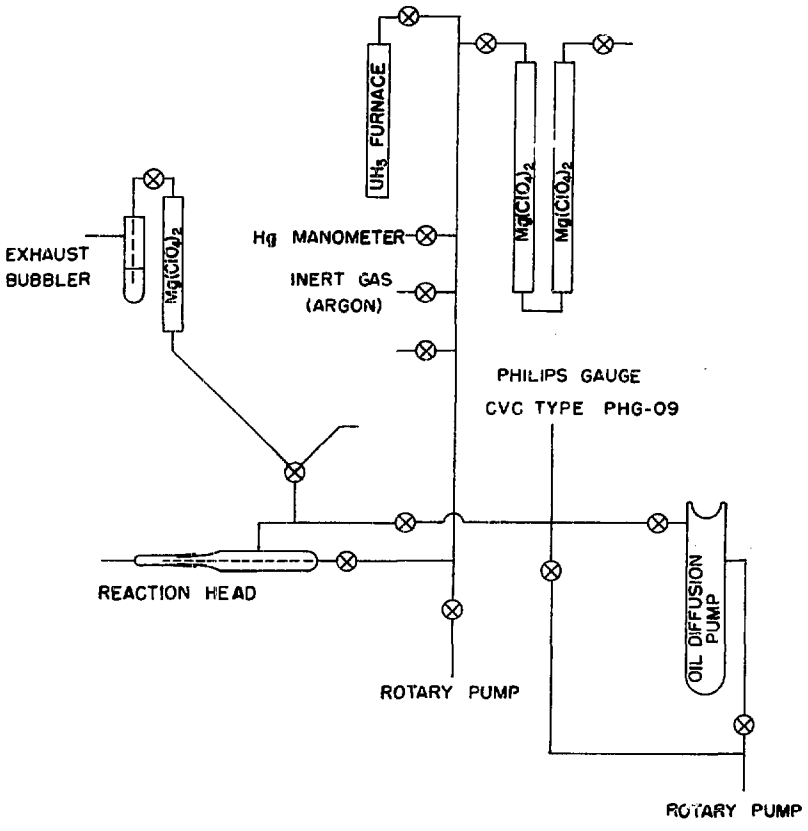

PREPARATIVE VACUUM LINE

XBL 725-802

Fig. XIV

to allow pure or mixed gases to be introduced to the area of the sample and then exhausted, either as a cycled or a continuous flow system. The actual point of introduction of any given gas into the line was determined by the character of the gas and the relative purity. Additional treatments of introduced gas were conducted as required and are noted in the discussion of the individual reactions. The total volume of the reaction head was about 50 ml.

X-ray analysis was carried out using the modified x-ray camera shown in Fig. XV. The lid of the camera was extended to allow clearance for the much longer than normal capillary and its support apparatus. The only substantial loss relative to the unmodified camera (a Debye-Scherrer type Norelco Precision Powder Camera) was the ability to rotate the sample through 360°, an oscillatory motion through approximately 100° being substituted.

The x-ray source used was a Jarrel-Ash Model 80-000 Microfocus unit fitted with a copper anode and an adjustable focus filament which produced a very intense beam, allowing small samples to be used without greatly increasing exposure time. All exposures were made in the modified 57.3 mm diameter camera described above using Ilford Industrial G x-ray film. A filter of 0.0035 inch Ni foil was placed either between the sample and the film or in the x-ray beam before it entered the camera to diminish the intensity of the CuK_β radiation. All film measurements were carried out on a Phillips-Norelco film reader capable of an accuracy of ±0.05 mm.

The resultant x-ray line lists were indexed either by analogy

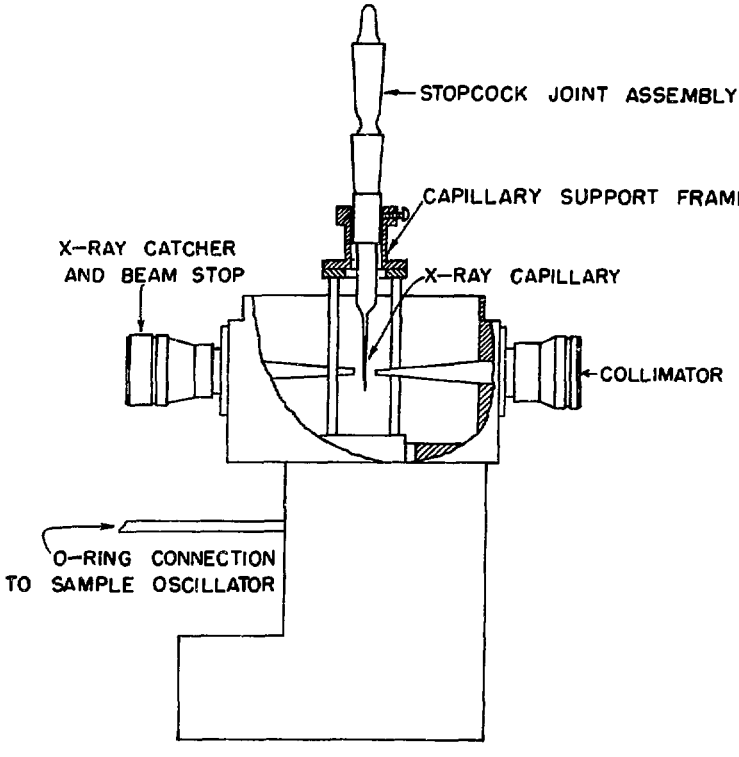

MODIFIED X-RAY CAMERA

XBL 725-808

Fig. XV

to line lists of isostructural compounds or by use of $\sin^2\theta$ and theoretical line intensities calculated by the computer programs POWD[28] and ANIFAC.[29] After indexing, the lattice parameters were calculated by least squares fitting with the program LCR-2 developed by D. E. Williams.[30] This program uses weighting factors of the form

$$w_i = \frac{\text{constant}}{\sin^2(2\theta_i)\sigma^2(\theta_i)}$$

where $\sigma(\theta_i)$ is the random error in the measurement of θ_1. $\sigma(\theta_i)$ was usually assigned the value 0.05°, the precision to which a line position could be measured with the film reader, but was occasionally given a larger value for lines which were the superposition of two or more lines or were exceptionally diffuse.

Error limits reported on all lattice parameters are standard deviations and represent only the internal consistency of the data for that particular preparation or x-ray diffraction film. Variation due to differences in stoichiometry or crystal defects between preparations commonly exceeds the error limits for internal consistency.

B. Results and Discussion

1. Reaction with oxygen.

Reactions were carried out successively at temperatures of 300, 500 and 700°C. Reaction for 1 hour at 300°C with oxygen which had been dried by passage through $Mg(ClO_4)_2$ produced a light gray or white powder. X-ray diffraction powder photographs showed only lines attributable to a fluorite type lattice, although they were quite broad and diffuse. The observed approximate lattice parameter was about 5.47 Å. The diffuse nature of the diffraction lines is consistent with the

reported tendency of low-fired oxides to be poorly crystallized,[31] and the cell volume is consistent with the pentoxide. The further reaction of the sample at 500°C yielded a product which was nearly identical in appearance and showed a very similar diffraction pattern with lines that were slightly sharper. Reaction for 1 hour at 700°C produced no change in the physical appearance, however, the broad lines of the low-fired oxides resolved into a sharp line pattern which was indexable on the basis of the Pa_2O_5 tetragonal lattice. The observed lattice parameters were $a_o = 5.421 \pm 3$ Å, $c_o = 5.492 \pm 4$ Å, values which are in reasonable agreement with those reported by Roberts and Walter for Pa_2O_5*. The apparent reaction of Pa metal with dry oxygen is therefore

$$2Pa + 5/2\ O_2 \longrightarrow Pa_2O_5$$

at all reaction temperatures checked.

2. Reaction with water vapor.

Pa metal was reacted with water vapor at 300 and 500°C. The gas for reaction was prepared by bubbling dry argon through distilled water at about 25°C, producing an atmosphere with a partial pressure of H_2O of approximately 25 torr. Because of the reduced relative amount of reactant gas in the reaction head, the gas was changed after each half hour of reaction by pumping out and renewing. After one half hour at 300°C, the metal sample had evidently lost some of its metallic luster, but there seemed to be metal still present. Reaction for a further half hour showed the sample to be gray-white in color and decomposing. X-ray analysis

---

*$a_o = 5.429 \pm 3$ Å, $c_o = 5.503 \pm 3$ Å (Ref. 31).

showed no signs of metal, only the fluorite type low-fired oxide with diffuse lines. Further reaction of the sample at 500°C in a similar manner produced no change in the physical appearance of the sample, however the x-ray diffraction pattern showed some sharpening of the lines as is characteristic of the pentoxide. The probable reaction of Pa metal with excess water vapor is therefore

$$2Pa + nH_2O \longrightarrow Pa_2O_5 + (n-5)H_2O + 5H_2 .$$

3. Reaction with carbon dioxide.

A sample of Pa metal was reacted with pure CO_2 at 300 and 500°C. The results were similar after both reactions, a sample of gray to white color and powdery in appearance which produced an x-ray powder pattern characteristic of cubic Pa oxides produced at low temperatures. The pattern taken after the reaction at 500° was somewhat sharper than that at 300°, and again characteristic of Pa_2O_5. The probable reaction of protactinium metal with CO_2 at 1 atmosphere pressure is therefore

$$2Pa + nCO_2 \longrightarrow Pa_2O_5 + (n - 5)CO_2 + 5CO.$$

4. Reaction with nitrogen.

A nitride of protactinium, "isostructural with uranium nitride," has been reported to be produced by the action of ammonia gas on either the pentachloride or tetrachloride of protactinium.[32] This compound was reported to be "a bright yellow solid not volatile in vacuum at 800°".[33] It was decided to attempt to confirm the existence of this compound by the reaction of protactinium metal with dry nitrogen and/or ammonia.

Nitrogen which had been dried by passage through the $Mg(ClO_4)_2$

columns was introduced to a pressure of 1 atmosphere into the reaction head and the x-ray capillary. The sample was reacted at 100°C for 1 hour, resulting in little change in the appearance of the sample. X-ray diffraction analysis showed the sample to be unchanged metal, although the lines were much more diffuse than before reaction. Reaction at 300°C under similar circumstances yielded a sample which although nearly unchanged in physical appearance, gave a diffraction pattern very similar to that of the oxides, but the lattice parameter was somewhat smaller (see Table 10). Further reaction of the sample at 500 and 700°C changed the appearance of the sample to a shiny black, but the diffraction pattern showed no change except for additional sharpening of the lines, although even at 700°, the lines were still quite diffuse, indicating poor crystallization.

Further heating of the sample in high vacuum (p <1 μtorr) produced no change in the physical appearance, although x-ray diffraction analysis showed the production of a second fluorite structure with a somewhat smaller unit cell, at first in conjunction with the original structure, and then as a replacement for it. No evidence was seen for the existence of any other protactinium nitride in reaction of the metal with nitrogen. Uranium nitride also exhibits a fluorite structure, but only in UN_2, a compound known to be produced only under high temperatures and high pressures of nitrogen.

A second metal sample, reacted with dry nitrogen in a similar manner at 200°C for 1 hour, changed from the silvery color of the metal to a bluish metallic color while retaining the same general appearance as the metal. An x-ray diffraction pattern of this sample

Table 10. Protactinium Nitride Lattice Parameters.

Sample #	Reaction temp.	Conditions	a_o, Å
1	300°C	N_2	5.443 ± 5
	500°C	N_2	5.448 ± 4
	700°C	N_2	5.445 ± 7
	700°C	vac.	5.398 ± 1
2	300°C	N_2	5.447 ± 6
	500°C	N_2	5.441 ± 5
	500°C	O_2	5.480 ± 3

indicated that approximately 80% of the sample was unreacted, while the remainder exhibited the larger fluorite structure attributed to the nitride. Further reaction of the sample at 300 and 500° produced a sample with the same dark steely appearance as the first sample, with the same crystal structure exhibited by that sample at these temperatures. Reaction of this sample for two hours in 1 atmosphere of dry oxygen yielded a white compound determined by x-ray analysis to be the "cubic" low-fired pentoxide.

Although there are no analytical data to support the supposition, it is likely that one of the two nitrides noted is the dinitride, PaN_2.

5. Reaction with ammonia.

In a further attempt to synthesize the bright yellow compound described by Sellers[33] and/or to confirm the existence of the fluorite-structured nitride observed in reactions with nitrogen, a series of reactions with ammonia gas which had been dried by passage through a column of CaO was carried out. Reactior for 1 hour at 100°C yielded a sample which was similar in appearance to the metal piece started with, although same loss of metallic luster was noted. X-ray diffraction analysis showed slight reaction to a fluorite structured compound of ca. 5.45 Å lattice constant, but the metallic phase still predominated. Further reaction at 300°C for 1 hour produced a sample of powdery appearance with a color of olive green. This proved to have a lattice constant of 5.43 Å, smaller than that of the comparable N_2-reacted sample (see Table 11). The quality of the diffraction pattern produced by this sample was quite poor, high angle lines being diffuse to the point

Table 11. Comparison of lattice parameters of protactinium nitrides prepared by reaction of Pa metal with nitrogen and ammonia.

Sample	Temperature, °C	a_o, Å
Pa + NH_3	300	5.431±6
	500	5.393±1
Pa + N_2	300	5.443±5
	700	5.398±1

to being absent. Reacting the sample again, this time at 500°C for 1 hour produced no apparent visual change from the green powder sample produced by reaction at 300°C. The x-ray powder photograph of this sample was superior in quality to that obtained from the same sample after reaction at 300° and the observed lattice constant was nearly identical to that observed from the nitrogen reaction sample which had been heated for several hours in high vacuum. The samples were different in physical appearance, however this could possibly be explained by an initial reaction on the ammonia with the metal yielding hydrogen which could then react with and powder the protactinium metal, which could then react with the ammonia, and so forth.

$$Pa + 2NH_3 \longrightarrow PaN_2 + 3H_2$$

$$Pa + 3/2H_2 \longrightarrow PaH_3$$

$$PaH_3 + 2NH_3 \longrightarrow PaN_2 + 9/2H_2$$

The powdering effect of the metal by formation of the hydride is well known with the isostructural uranium hydrides and was observed with protactinium in reaction with hydrogen, a reaction which shares with the corresponding uranium a large change in molar volume.

The line list of the compound produced by reaction with ammonia gas at 500°C is shown in Table 12.

6. Reaction with air.

Of greatest interest in the interaction of protactinium metal and air is the effect on the metal at room temperature. Although protactinium has been reported to be oxidized by air at room temperature, metal samples prepared prior to this series of experiments have been allowed to remain

Table 12. Line list and indexing for CaF_2-type Pa nitride prepared by reaction of Pa metal with ammonia at 500°C. (Film no. 4187A)

Miller Indices hkl	Observed spacing (Å)	Observed 2θ (degrees)	Calculated 2θ* (degrees)	Observed Line Intensity**
111	3.100	28.80	28.67	10
200	2.698	33.20	33.22	5
	2.117	42.71		(v)***
220	1.907	47.68	47.70	8
	1.803	50.61		(v)***
311	1.623	56.72	56.60	9
222	1.560	59.22	59.36	3
400	1.347	69.82	69.75	3
	1.249	76.23		1***
331	1.235	77.23	77.08	4
420	1.206	79.43	79.48	3
422	1.100	88.93	88.90	3
	1.059	93.44		1***
511	1.037	96.04	95.94	3
531	0.9112	115.55	115.49	4
600	.8995	117.95	118.12	2
620	.8528	129.36	129.40	3

(v) = visible, but very low intensity

*calculated from least-squares fit of data using program LCR-2 (Ref. 30)

**visually estimated, most intense line = 10

***lines observed but not indexable

in contact with air for a period of several months with little or no appreciable tarnishing. To reach a more quantitative conclusion, a clean metal x-ray sample was allowed to sit in its capillary in laboratory air for a period of five days at room temperature (ca. 25°C). There was no visually apparent change in the sample at the end of that period, and x-ray diffraction analysis showed only the unreacted metal to be present. The sample was then reacted in air for 1 hour at 100°C. A slight loss of metallic luster was visually apparent, but the x-ray diffraction pattern showed the metal sample to be still essentially unreacted. Reaction at 300°C for 1 hour caused the sample to turn grayish-white and begin to disintegrate. The x-ray diffraction pattern of this sample exhibited the diffuse lines of a fluorite structure ($a_o \approx 5.48$ Å) which are characteristic of the low-fired oxides of protactinium. Further reaction of the sample at 500°C for 1 hour produced no significant change in either its physical appearance or the x-ray diffraction pattern yielded. Apparently, therefore, the metal reacts with the oxygen and/or water vapor in laboratory air to form a pentoxide, although the rate of reaction does not become significant until temperatures greater than 100°C are reached.

It is worthy of note at this point that neither in this reaction sequence nor in any other in this study was any sign of the monoxide, PaO, observed, although this compound is reportedly formed when a metal sample is exposed to air.[33] While the new observation does not preclude the existence of such a compound, it does cast considerable doubt on the report which is based on early work with small quantities of the metal. Further, although lines ascribable to the fluorite-structured higher oxides of protactinium have been observed not uncommonly in the many x-ray

patterns taken of the metal in this laboratory recently, no lines identifiable as the monoxide have been noted. Also, the recently reported face-centered cubic phase of the metal[16] possesses a structure which is very similar to that reported for the monoxide, with a unit cell of nearly identical size.

7. Reaction with hydrogen.

Perhaps one of the more interesting reactions to investigate is that of protactinium metal with pure hydrogen, since protactinium metal is quite unreactive with respect to most mineral acids and, thus, enthalpies of formation of protactinium compounds cannot currently be calculated even though some solution calorimetry has been carried out on compounds of protactinium.[34] Since actinide hydrides tend to be quite reactive, measurements of the equilibrium dissociation pressure of hydrogen over protactinium hydride coupled with the heat of solution of the hydride would serve to circumvent the lack of direct heat of solution measurements on the metal.

A hydride of protactinium was reported to be formed by the addition of hydrogen to protactinium metal at 250°C.[33] This compound was determined to be isostructural with β-uranium hydride. No further study of the hydride of protactinium has been reported.

Samples of protactinium metal were exposed to hydrogen generated by the thermal decomposition of uranium hydride. In order to avoid formation of a hydride phase characteristic of a lower temperature and to avoid thermal decomposition of the existing hydride, the furnace was removed from the capillary simultaneously with the evacuation of the

sample area following reaction. A sequence of reactions was carried out at 100°, 200° and 300°C in 1 atmosphere of hydrogen, producing in each case a gray, powdered substance. This was identified by x-ray diffraction analysis as a compound isomorphic with α-uranium hydride, a different structure than that reported by Sellers for protactinium hydride. The observed lattice parameters are shown in Table 13, with sample line listings in Tables 14 and 15. Further reaction at 400°C in 1 atmosphere of hydrogen led to the formation of a compound of similar physical appearance, but which yielded an x-ray diffraction pattern which has not yet been identified. An unindexed line list for that diffraction pattern is shown in Table 16. Subsequent reaction of the same sample at 400°C in 1/2 atmosphere of hydrogen produced no change in the physical appearance of the sample, but the x-ray pattern of this sample showed it to be returned to the metallic state, tetragonal phase, with two of the most intense lines of the unidentified hydride pattern still present, but in very low intensity. This transformation clearly indicated that the unidentified compound represents some hydride of protactinium, since such thermal decomposition to the metal is not known for any other protactinium compounds at this temperature. At no time in this series of experiments did any sample exhibit the β-uranium hydride structure which was reported previously.

Protactinium hydride proved to be similar to the hydrides of the higher actinides in that it is very reactive, and several samples were lost in preparation by the formation of oxide from some leakage in the x-ray capillary - reaction chamber.

Table 13. Summary of protactinium hydride lattice parameters.

Sample No.	Reaction Temp.	Lattice Type	Lattice Constants
1	100°C	Cubic	a_o = 4.150±2 Å
2	200°C	Cubic	a_o = 4.150±3 Å
3	300°C	Cubic	a_o = 4.154±2 Å
3	400°C	?	?

Table 14. Powder pattern of PaH_3 prepared by reaction of Pa metal with hydrogen at 100°C and 1 atm. pressure. (Film no. 3930A)

Miller Indices, hkl	Interplanar spacing, d(Å) (observed)	Line position, 2θ(degrees) Observed	Calculated[a]	Intensity, estimated[b]
110	2.929	30.52	30.46	10
200	2.066	43.82	43.62	4
211	1.689	54.31	54.13	7
220	1.467	63.41	63.39	3
310	1.311	72.00	71.95	4
222	1.197	80.20	80.10	1
321	1.108	88.20	88.06	4
411,330	0.9777	104.09	104.02	3
420	.9300	111.98	112.35	2

[a]Calculated from LCR-2, least-squares fitting program for $a_o = 4.150 \pm 2$ Å.

[b]Visually estimated, most intense line = 10.

Table 15. Powder pattern of PaH_3 prepared by reaction of Pa metal with hydrogen at 300°C and 1 atm. pressure. (Film no. 3956A)

Miller Indices, hkl	Interplanar spacing, d(Å) (observed)	Line position, 2θ(degrees) Observed	Calculated[a]	Intensity, estimated[b]
110	2.927	30.54	30.43	10
200	2.074	43.64	43.58	3
211	1.697	54.04	54.08	6
220	1.470	63.24	63.32	2
310	1.313	71.94	71.87	3
321	1.111	87.84	87.87	3
411,330	0.9788	103.94	103.88	2

[a]Calculated from LCR-2, least-squares fitting program for $a_o = 4.154 \pm 2$ Å.

[b]Visually estimated, most intense line = 10.

Table 16. Unidentified powder pattern of reaction product of Pa metal and hydrogen at 400°C and 1 atm. pressure. (Film no. 3958A)

Intensity, estimated	Interplanar spacing, d(Å)	Line position, 2θ (degrees)
2.5	3.293	27.08
10	2.811	31.82
5	2.694	33.24
2.5	1.903	47.79
8	1.794	50.91
8	1.650	55.75
2(b)*	1.478	62.91
2.5	1.427	65.41
4	1.409	66.35
1	1.249	76.23
7	1.217	78.73
1	1.171	82.41
1	1.101	89.91
4(b)	1.078	91.37
3(b)	0.9779	104.05
4(b)	.9290	107.86
5(b)	.9003	117.30

*(b) indicates a diffuse line

The most probable reaction of protactinium with hydrogen at temperatures below 400°C is

$$Pa + 3/2H_2 \longrightarrow PaH_3$$

as is indicated by the product being isomorphic with UH_3. The product of reaction of hydrogen with protactinium at 400°C is not clearly indicated from the product x-ray pattern, and the constraints of the reaction system did not allow for other determination of stoichiometry.

8. Reaction with hydrogen chloride gas.

Since the pentavalent halides of protactinium are known to be volatile at relatively low temperatures,[33,35-43] reactions of the metal with hydrogen halide gases were conducted at lower maximum temperatures than other gases to avoid loss of sample through vapor transport from the hot area of the capillary.

Pure HCl gas (Matheson) was admitted to the system through columns of $Mg(ClO_4)_2$ to remove any residual water. The sample was heated to 100°C and 1 atmosphere of HCl gas was admitted. The gas was removed and replaced with new at 15 minute intervals, and at the same time the physical appearance of the sample was checked. Following 1 hour of reaction at 100°C, the sample was removed again from the furnace. No visible change was apparent in the metal, although there seemed to be a very small amount of light colored condensate on the inside of the capillary near the sample. X-ray diffraction analysis showed only the pattern of the metal, although the area of capillary containing the condensate was also in the beam. Further reaction in the same manner at a temperature of 300°C produced a dark mass, no longer metallic, which

transmitted yellow-green light at the edges. X-ray analysis of the sample showed it to be predominantly $PaCl_4$ with a minor phase which could be attributed to oxide, presumably due to some small leakage in the system. This result is consistent with the yellow-green color reported for $PaCl_4$.[43] The reaction of protactinium metal with hydrogen chloride gas would therefore be

$$Pa + nHCl \longrightarrow PaCl_4 + 2H_2 + (n-4)HCl$$

at 300°C. The only evidence for the existence of the volatile pentachloride found in this reaction was the small amount of condensate noticed in the reaction at 100°C. The condensate could be $PaCl_5$ which is reported to be volatile in vacuo at 160°C.[37] In any event, the amount of condensate was too small to permit analysis and would certainly constitute a very minor phase.

9. Reaction with hydrogen bromide gas.

Hydrogen bromide was introduced into the system through a tube filled with granular NaBr which was maintained at ca. 500°C to scavenge any lighter halides which might be present in the gas. It was then dried in the usual manner by passage through columns of $Mg(ClO_4)_2$. The metal sample was heated to 100°C and treated with 1 atmosphere of HBr for 1 hour, with the gas removed and renewed at 15 minute intervals. Microscopic examination of the sample following this procedure showed the metal sample to be essentially unchanged except in color, there being an orange cast present instead of the pure silvery appearance of the unreacted metal. The x-ray powder pattern showed only metal to be present, but the intensity of the lines was reduced from that observed before reaction, as

if an additional scattering layer were introduced into the beam, a layer with insufficient crystallinity to show diffraction lines.

The sample was returned to the vacuum line and reaction with HBr was commenced at 200°C, the gas again being changed at 15 minute intervals. At the second change of gas (30 minutes at 200° in 1 atmosphere of HBr gas), relatively large orange needles (~0.05 mm long) were observed to be forming at the edge of the hot zone in the capillary. The bulk of the sample had taken on an orange-yellow color and appeared to be partially melted. The reaction was terminated at that point and the capillary evacuated for x-ray analysis.

No useable diffraction pattern was obtained from the sample as it was no longer polycrystalline enough to satisfy the requirements of the powder method. Instead, a series of spots, as from one or more single crystals, was observed. Assignment of the observed spots to a known structure proved impossible, although the color indicated that the product was probably the oxydibromide, $PaOBr_2$, at least in part. Other oxybromides of protactinium[41] and the tetrabromide[35] are all of colors which can rule them out as possible identities of the product. The probable source of oxygen in this compound is traces of air admitted with the HBr gas.

Since $PaOBr_2$ is readily formed from $PaBr_4$ at these temperatures,[44] and the expected effect of oxygen on a protactinium bromide would be oxidation of +5 if it were not already in that oxidation state, the probable reaction of protactinium metal with HBr gas at 200°C is

$$Pa + nHBr \longrightarrow PaBr_4 + (n-4)HBr + 2H_2,$$

a reaction which in this case was followed at least partially by further

reaction

$$PaBr_4 + \frac{1}{2}O_2 \longrightarrow PaOBr_2 + Br_2.$$

The simultaneous reaction of the metal with both oxygen and HBr

$$Pa + \frac{1}{2}O_2 + nHBr \longrightarrow PaOBr_2 + H_2 + (n-2)HBr$$

cannot, of course, be ruled out.

Further study of this reaction should be made in order to draw firm conclusions.

10. Reaction with hydrogen iodide gas.

HI gas was introduced through a column of NaI which was held at ca. 500°C to scavenge any lower halides from the gas stream. The gas was then dried by passage through anhydrous $Mg(ClO_4)_2$ columns.

Reaction for 1 hour at 100°C in 1 atmosphere of HI produced no visible change in the sample, an observation supported by the x-ray diffraction pattern which showed no change from the metal. Further reaction at 200°C showed again no change in the physical appearance of the sample, although a light colored film had condensed inside the capillary somewhat removed from the sample. X-ray analysis confirmed that the sample was primarily metal, although there was some evidence for a second, unidentified phase beginning to appear. Further reaction at 300°C for 1 hour yielded a dark sample which appeared to have wet the quartz of the capillary. An orange film was visible inside the capillary near the edge of the hot zone. The x-ray diffraction pattern of the bulk of this sample was of very poor quality, the few lines visible being very grainy in nature, indicating macrocrystallinity of the sample. The observed lines could not be indexed as any known iodide or oxyiodide of protactinium,

although the physical appearance is consistent with that of PaI_5.[39,40,43]

V. THERMAL EXPANSION BEHAVIOR OF PROTACTINIUM METAL

A recent report was made[45] of the thermal expansion behavior of protactinium metal. The experimental data from that report showed a small positive volume coefficient of thermal expansion and extrapolated to a convergence from body-centered tetragonal to body-centered cubic at approximately 1200°C, a convergence which could not be confirmed due to "rapid surface oxidation of the specimen". This statement that the experiment was performed under conditions in which the specimen could be readily oxidized, coupled with the studies of the reaction of Pa metal with air, caused question to arise as to whether the expansion of the metal was retarded by a thin oxide layer formed at lower temperatures. Further, Marples' sample of protactinium metal contained "some" niobium and "probably some" copper. The copper was estimated by Marples to be approximately 1% and the original protactinium stock contained approximately 4% niobium.

A. Experimental

The experiments described here utilized a new type of high temperature x-ray powder camera initially described by Fujita.[46] This was a standard 57.3 mm diameter Debye-Scherer type Norelco Precision Powder Camera manufactured by Phillips Electronic Instrument Co. which was modified as described in Sec. IV to allow vertical positioning of sample capillaries and then further modified by the addition of a heating coil directly around the sample (Fig. XVI). With this camera, it was possible to attain temperatures as high as 600°C at the sample position for short periods of time, and to maintain temperatures up to 500°C for a period of

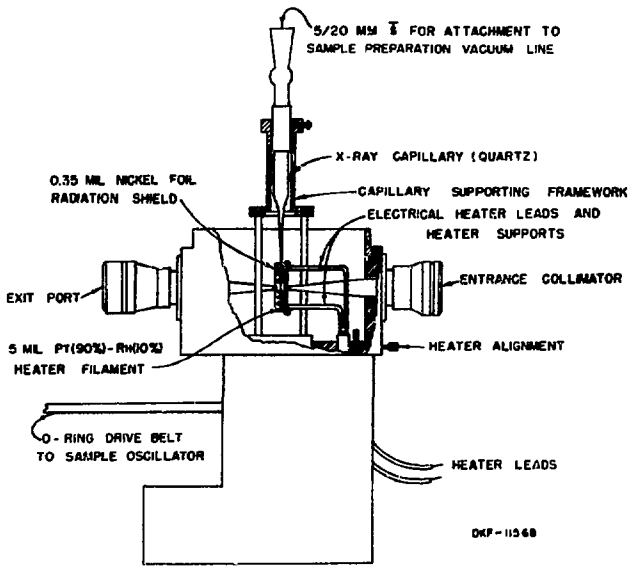

Fig. XVI. Modified x-ray camera with heating filament.

hours inside the closed diffraction camera without causing excessive temperature rise in the area of the film. The nickel shield which surrounded the heating coil acted as a chimney guiding the heated air surrounding the capillary up and directing it into the extended cap where the brass lid conducted the heat harmlessly to the outside and dissipated it. It was necessary with the camera so modified to wrap the film in some sort of light-tight material to avoid fogging of the film by the light from the coil, which has an appreciable glow at sample temperatures of 500°C and above; in these experiments, a piece of 0.00035 inch nickel foil was used as the wrapping material, providing an additional degree of filtering of the Cu K radiation from the diffracted x-rays.

The camera heater was supplied low-voltage, diode-rectified a-c current through a Variac, and the filament current was monitored as a temperature indication. Calibration was carried out using substances of well-defined, known melting points mounted as the protactinium specimen was in fine quartz capillaries. The melting of the temperature standard substances was observed by telescope through the x-ray catcher tube with the beam-stop window removed. A sample calibration curve is shown in Fig. XVII. The calibration of the camera heater was checked after the protactinium specimens were removed from the camera and it was found to be unchanged.

Two samples of pure protactinium metal were prepared from the two metal samples used for magnetic susceptibility studies. These were loaded into quartz capillaries drawn from standard taper joints. After degassing at 700°C under a vacuum of 1 μtorr, the metal samples were sealed off,

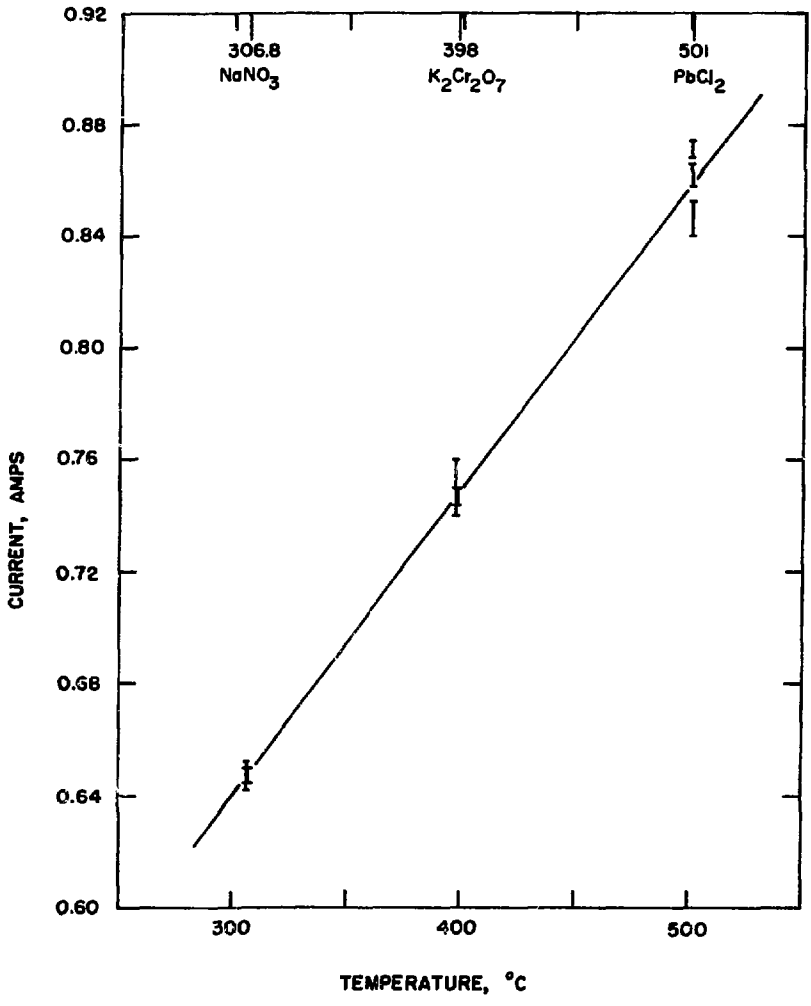

Fig. XVII. Temperature calibration of high-temperature x-ray camera.

still under vacuum, in short lengths of capillary. These capillaries were then mounted in a length of quartz tubing with Sauereisen cement to avoid any shifting of the sample during an exposure at high temperature. The quartz tubing was similarly fitted with a brass collar to allow mounting in the modified x-ray powder camera.

B. Results and Discussion

X-ray powder diffraction photographs were taken of each sample at room temperature (approximately 30°C) as well as at 300°C and 500°C. The lattice parameters calculated from these photographs are tabulated in Table 17.

As can be seen in Fig. XVIII, basic agreement exists with the previously reported results, although a somewhat smaller value of the c_o parameter could indicate a higher projected temperature of convergence to the body-centered cubic structure for the pure metal.

Although the second specimen was prepared in anticipation of observing the thermal expansion behavior of the face-centered cubic phase of the metal, the preliminary degassing at 700°C for an hour was evidently sufficient to anneal out any of the high-temperature phase left after cutting of the specimen.

The average volume coefficient of thermal expansion over the range studied for protactinium amounts to only 18×10^{-6}/°C, considerably less than that shown by the neighboring elements (see Table 18). The reason for this is not clear, but considering the disagreement over the metallic valence of protactinium,[18,47,48] a possible explanation could lie in an increasing participation of the f electron in bonding as the tempera-

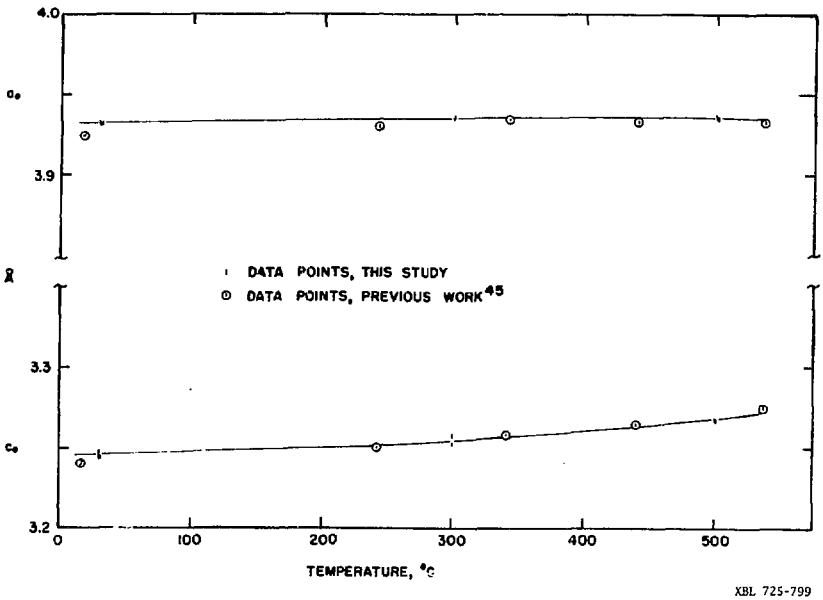

Fig. XVIII. Thermal expansion behavior of protactinium metal.

Table 17. Protactinium Lattice Parameters

Sample #1*			Sample #2**		
temp., °C	a_o, Å	c_o, Å	temp., °C	a_o, Å	c_o, Å
30	3.931±1	3.248±1	30	3.931±1	3.244±1
300	3.936±1	3.253±1	300	3.934±1	3.258±1
500	3.936±1	3.268±1	500	3.935±1	3.267±1
30	3.932±1	3.244±1			

*from magnetic susceptibility sample #1

**from magnetic susceptibility sample #2

Table 18. Expansion of Thorium, Protactinium, and Uranium

temp., °C	atomic volume, $Å^3$		
	Th(Ref. 53)	Pa	U(Ref. 54)
20	32.850	25.09_5	20.75
100	32.948	25.12	20.81
200	33.072	25.15	20.92
300	33.196	25.19_5	21.02
400	33.321	25.26	21.13
500	33.445	25.30	21.28
average coefficient of volume expansion /°C × 10^6	38	18	54

temperature increases, an effect postulated to cause the negative coefficient of expansion in δ-plutonium.[47,49]

VI. MELTING POINT OF PROTACTINIUM METAL

The melting point of protactinium metal has been previously reported to be 1560±30°C (8) and 1575±20°C (45). Although these values are in reasonable agreement, it was felt to be worthwhile to attempt to refine the value with metal of known purity, since the metal samples used in previous determinations were of unstated purity.

In the preparation of the metal for this experiment, the older method utilizing a tungsten wire spiral for support of the protactinium fluoride during reduction was used. A metal sample resulting from this preparation was found to be bridged between two adjacent loops of the spiral, wetting and enveloping the wire at both points of contact (Fig. XIX). The wire was cut at point (b) and the sample suspended from point (a) with a weight attached at point (c). The sample was hung in a double tantalum shield system as shown in Fig. XX which was heated inductively. The temperature was monitored with an optical pyrometer, reading the temperature of the inner chamber through small holes punched in the shield walls. With the sample so suspended, the melting point was recorded as that point at which the weight fell free, indicating failure of the "soldered" joint. The system allowed the weight to drop completely free of the shields, carrying a small portion of the protactinium metal quickly to a cooler area of the vacuum line. In this way, it was attempted to duplicate the results reported by Cunningham[8] in which he reported an unidentified high-temperature crystal structure for the metal. No structure other than the normal room-temperature tetragonal phase was observed in this experiment.

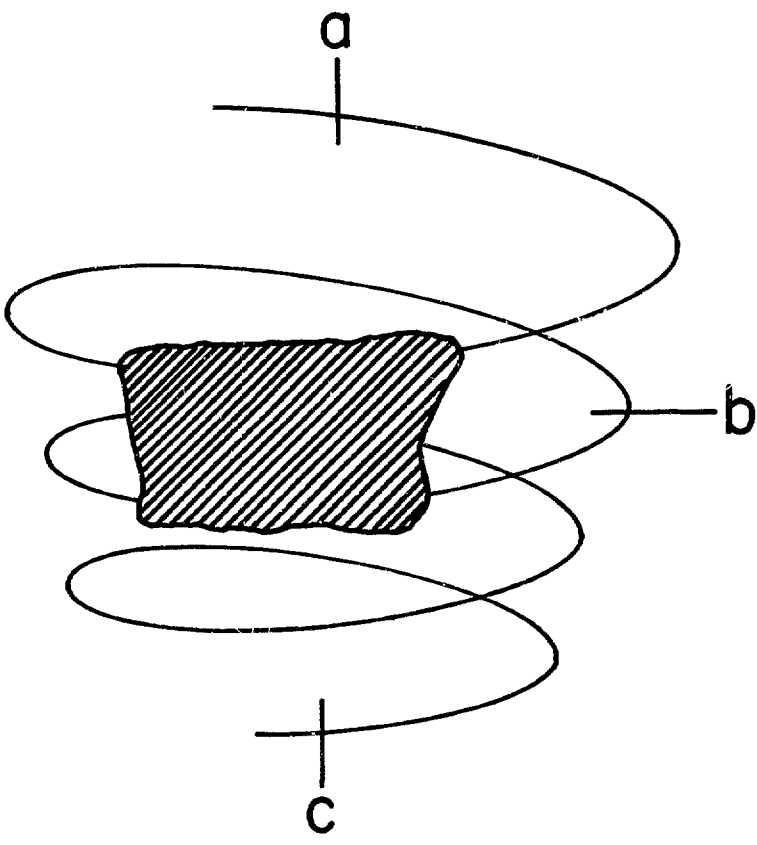

XBL 725-800

Fig. XIX. Metal sample for melting point determination.

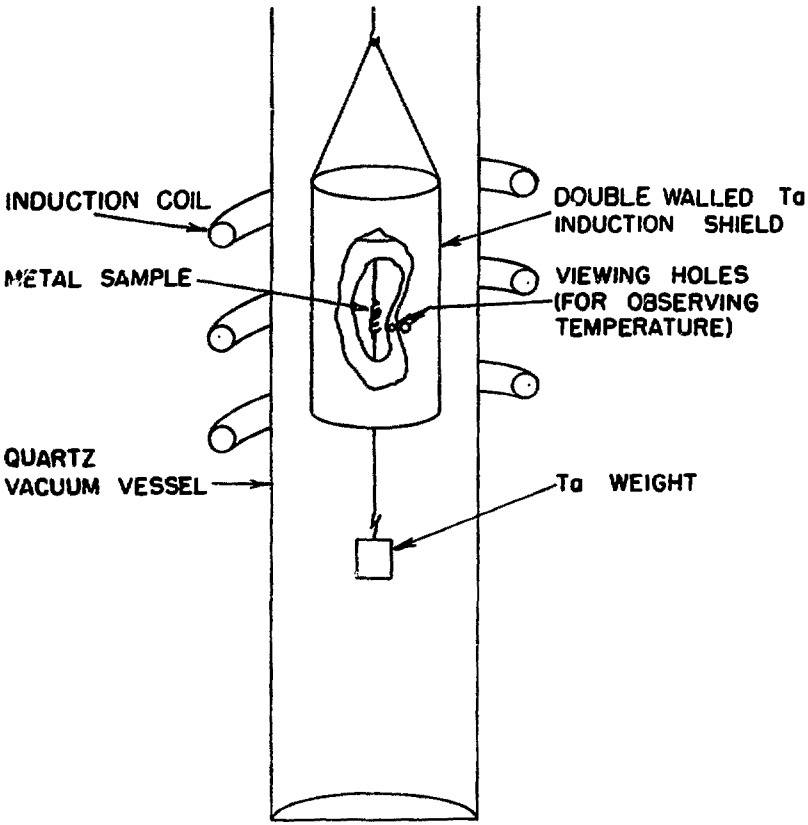

XBL 725-804

Fig. XX. Apparatus for measuring metal melting point.

The single value of the melting point of protactinium metal obtained here, 1562 ± 15°C, was in good agreement with the previously reported values. However, the alloying behavior of Pa metal with tungsten which was later observed places this value, and the previous value reported by Cunningham (which was determined in a similar manner) in a position of doubtful certainty, since alloy formation would most likely affect the melting point observed for the metal. Since the other previous melting point determination was of metal of doubtful purity (1% Cu, "some" Nb), a redetermination of the melting point of pure protactinium metal should be made.

ACKNOWLEDGMENTS

I wish to express my thanks to the many people without whose assistance the research for this dissertation could not have been concluded.

The late Professor Burris Cunningham, at whose suggestion and under whose direction the work was begun and largely carried out was primary among these. His unique skills as an experimentalist were inspiring to watch and to learn from.

Tom Parsons, who designed much of the specialized equipment used in the studies described here, provided assistance and advice in its use, and helped with hours of thoughtful discussion, was essential to the completion of the research.

Dennis Fujita and Lester Morss also provided many hours of assistance and discussion through the period of this work. Norman Edelstein provided advice on the magnetic measurements.

The assistance of the Lawrence Berkeley Laboratory Safety Services department, so necessary for any work with radioactive materials, is gratefully acknowledged, in particular the radiological monitoring assistance of Gerda Bolz, whose nerves I must have tried in the extreme at times, and Diane Gowdy.

Lillian Hill and Lilly Goda provided much needed general laboratory assistance. George Shalimoff and Ralph McLaughlin ran the many spectroscopic analyses needed at so many points in the purification and preparation of materials.

The advice of Profs. Leo Brewer, Alan Searcy and Neil Bartlett

who read and corrected this thesis is greatly appreciated.

Countless others among the support groups at the Lawrence Berkeley Laboratory have in many ways made this work possible.

I wish especially to thank my wife, Anne, for her moral support throughout the course of my graduate studies. Without her patience and understanding this work would not have been possible. Special thanks also go to my parents, for their continuous support and encouragement from the earliest times.

This work was done under the auspices of the United States Atomic Energy Commission.

REFERENCES

1. K. Fajans, Ber., 46, 422 (1913).
2. K. Fajans, Phys. Z., 14, 126 (1913).
3. K. Fajans, Radium, 10, 61 (1913).
4. A. S. Russell, Chem. News, 107, 49 (1913).
5. A. Von Grosse, Naturwiss., 15, 766 (1927).
6. A. Von Grosse, Nature, 120, 621 (1927).
7. D. A. Collins, J. J. Hillary, J. S. Nairn and G. M. Phillips, J. Inorg. Nucl. Chem., 24, 441 (1962).
8. B. B. Cunningham, Physico-Chimie du Protactinium, (Editions du Centre National de la Recherche Scientifique, Paris, 1966), p. 45.
9. A. Chetham-Strode and O. L. Keller, ibid., p. 189.
10. R. C. Petterson, University of California, Lawrence Radiation Laboratory Report, UCRL-11074 (1963).
11. D. Brown, S. N. Dixon, K. M. Glover and F. J. G. Rogers, J. Inorg. Nucl. Chem., 30, 19 (1968).
12. C. M. Lederer, J. M. Hollander and I. Perlman, Table of Isotopes, 6th Edn., (John Wiley and Sons, Inc., N.Y., 1967).
13. R. B. Ellis and W. S. Wilcox, Second Conference on Nuclear Reactor Chemistry, USAEC report TID-7622, p. 128 (1961).
14. R. D. McLaughlin, private communication (1969).
15. B. M. Bansal, (Ph.D. Thesis), University of California Lawrence Radiation Laboratory Report, UCRL-16782 (1966).
16. L. B. Asprey, R. D. Fowler, J. D. G. Lindsay, R. W. White and B. B. Cunningham, Inorg. Nucl. Chem. Letters, 7, 977 (1971).

17. B. B. Cunningham, J. Chem. Educ., 36, 31 (1959).

18. L. H. Bates, Modern Magnetism, 4th Edn., (Cambridge University Press, London, 1961).

19. L. Stein, Inorg. Chem., 3, 995 (1964).

20. P. Handler and C. A. Hutchinson, J. Chem. Phys., 37, 1210 (1956).

21. C. A. Hutchinson, Tung Tsang and B. Weinstock, J. Chem. Phys., 37, 555 (1962).

22. M. E. Hendricks, E. R. Jones, Jr., J. A. Stone and D. G. Karraker, J. Chem. Phys. 55, 2993 (1971).

23. J. L. Green, (Ph.D. Thesis), University of California, Lawrence Radiation Laboratory Report, UCRL-16516 (1965).

24. J. R. Peterson, (Ph.D. Thesis), University of California, Lawrence Radiation Laboratory Report, UCRL-17875 (1967).

25. J. C. Copeland, (M.S. Thesis), University of California, Lawrence Radiation Laboratory Report, UCRL-17718 (1967).

26. D. K. Fujita, (Ph.D. Thesis), University of California, Lawrence Radiation Laboratory Report, UCRL-19507 (1969).

27. T. C. Parsons, private communication (1969).

28. D. K. Smith, University of California, Lawrence Radiation Laboratory Report, UCRL-7196 (1963).

29. A. C. Larson, R. B. Roof, Jr., and D. T. Cromer, Los Alamos Scientific Laboratory Report, LA-3335 (1965).

30. D. E. Williams, Ames Laboratory Report, IS-1052 (1964).

31. L. E. J. Roberts and A. J. Walker, Physico-Chimie du Protactinium, (Editions du Centre National de la Recherche Scientifique, Paris, 1966), p. 51.

32. P. A. Sellers, S. Fried, R. E. Elson and W. H. Zachariasen, USAEC Report, AECD-3167 (1951).

33. P. A. Sellers, S. Fried, R. E. Elson and W. H. Zachariasen, J. Amer. Chem. Soc., 76, 5935 (1954).

34. J. Fuger, J. Chem. Soc. (A), 1970, 763.

35. D. Brown, T. J. Petcher and A. J. Smith, J. Chem. Soc. (A), 1971, 908.

36. D. Brown, T. J. Petcher and A. J. Smith, Acta Cryst., B25, 178 (1969).

37. D. Brown and A. G. Maddock, Quarterly Reviews XVII, No. 3, 289 (1963).

38. D. Brown and J. F. Easey, J. Chem. Soc. (A), 1970, 3378.

39. D. Brown, J. F. Easey and P. J. Jones, J. Chem. Soc. (A), 1967, 1698.

40. V. Scherer, F. Weigel and M. Van Ghemen, Inorg. Nucl. Chem. Letters 3, 589 (1967).

41. D. Brown and P. J. Jones, J. Chem. Soc. (A), 1966, 262.

42. A. Von Grosse, J. Amer. Chem. Soc., 56, 2200 (1934).

43. D. Brown and P. J. Jones, J. Chem. Soc. (A), 1967, 719.

44. K. W. Bagnall, D. Brown and J. F. Easey, J. Chem. Soc. (A), 1968, 288.

45. J. A. C. Marples, Acta Cryst., 18, 815 (1965).

46. D. K. Fujita, Inorg. Nucl. Chem. Letters 5, 307 (1969).

47. W. H. Zachariasen, The Metal Plutonium, (The University of Chicago Press, Chicago, 1961), p. 99.

48. B. B. Cunningham, J. Inorg. Nucl. Chem., 26, 271 (1964).

49. K. A. Geschneidner, Acta Metallurgica, 11, 947 (1963).

50. D. B. McWhan, B. B. Cunningham and J. C. Wallmann, J. Inorg. Nucl. Chem. 24, 1025 (1962).

51. P. Cossee, J. Inorg. Nucl. Chem., 14, 127 (1960).

52. J. K. Dawson, J. Chem. Soc., 1951, 2889.

53. J. F. Smith, Proceedings of the Conference on the Metal Thorium, Cleveland (1956).

54. L. T. Lloyd and C. S. Barrett, J. Nucl. Materials, 18, 55 (1966).

55. For the structure of isomorphic UF_4, see A. C. Larson, R. B. Roof and D. T. Cromer, Acta Cryst. 17, 555 (1964).